Synchronization and multi-frequency oscillations in the low-dimensional chain of the self-oscillators.

Emelianova Yu.P.[1], Kuznetsov A.P.[2], Sataev I.R.[2], Turukina L.V.[2]

[1] *Department of Electronics and Instrumentation, Saratov State Technical University, Polytechnicheskaya 77, Saratov 410054, Russian Federation.*

[2] *Kotel'nikov's Institute of Radio-Engineering and Electronics of RAS, Saratov Branch, Zelyenaya 38, Saratov, 410019, Russian Federation.*

The problem of growing complexity of the dynamics of the coupled phase oscillators as the number of oscillators in the chain increases is considered. The organization of the parameter space (parameter of the frequency detuning between the second and the first oscillators versus parameter of dissipative coupling) is discussed. The regions of complete synchronization, quasiperiodic regimes of different dimensions and chaos are identified. We discuss transformation of the domains of different dynamics as the number of oscillators grows. We use the method of charts of Lyapunov exponents and modification of the method of the chart of dynamical regimes to visualize two-frequency regimes of different type. Limits of applicability of the quasi-harmonic approximation and the features of the dynamics of the original system which are not described by the approximate phase equations are discussed for the case of three coupled oscillators.

Keywords: synchronization, phase oscillators, quasi-periodic dynamics, chaos.

Mathematics Subject Classification: 39Axx, 93D05

Introduction

In the theory of oscillations and nonlinear dynamics there is a fundamental problem concerning dynamics of coupled self-oscillators [1-9]. Coupled oscillators are common in radio-physics, electronics, biophysics, chemistry and etc. [1-18]. The system of coupled van der Pol oscillators is probably the simplest one [1-5]. Such models as Brusselator [10-11] and electronic oscillators [3,15-18] are also widely investigated.

Note, that two coupled self-oscillators demonstrate a very complex picture of the possible effects and this complexity still continues to evolve as our understanding becomes deeper. There are classical effects such as mode-locking of the oscillators with different ratios of the frequencies and two-frequency quasi-periodic regimes. In the case of dissipative coupling the “oscillator death” is also possible [1, 19]. This effect is observed experimentally in the system of coupled electronic [20], optical [21], chemical [22, 23], biological [24] and etc. oscillators. Quasi-harmonic approximation and phase equations approach was used in [25] to study the effects of the combined dissipative and reactive types of coupling, the case of coupled oscillators with nonidentical control parameters was considered in [26], while non-isochronism of the oscillators was taken into account in [27]. Some effects of the synchronization picture such as multistability, chaos and non-isochronism were discussed in [28-33]. In a series of the works such factors as nonlinear coupling [34, 35], “delay coupling” [36, 37], coupling “via a bath” [38], and etc. were considered

too. Bifurcations of different regimes of the coupled oscillators were investigated in detail in [3, 39].

Such a wide field of research is due to a variety of physical effects and mechanisms, as well as the fact that the dynamics of a system of coupled oscillators can be discussed at different levels. For example, we can study directly the dynamics of the original system, the quasi-harmonic approximation for the slow complex amplitude and finally the phase approximation equations.

The problem of studding the three-frequency quasi-periodic dynamics (for example, two driven coupled oscillators or three coupled oscillators) is more complex and many-sided. In one of the most fundamental work [40] a system of two coupled rotation maps is discussed as a model of coupled oscillators. The frequency detuning parameters plane is analyzed and a variety of bifurcations observing in coupled maps is discussed. Experimental studies of three-frequency quasi-periodicity in coupled electronic oscillators were carried out in [41]. In [42] the authors investigated a model of two van der Pol oscillators with reactive coupling excited by an external periodic force. For weak coupling and small amplitude of external force the dominant three-frequency quasi-periodicity was observed, and in the case of large coupling chaotic behavior becomes possible and typical. Three coupled oscillators were studied theoretically in [43-45], and experimental study of electronic device was described. The authors showed that saddle-node bifurcation of stable and unstable two-frequency tori lead to the three-frequency quasi-periodicity. In [46, 47] the authors investigated three-frequency quasi-periodicity and transition to chaos in the system of three coupled Lorentz system. Three coupled van der Pol oscillators with reactive type of coupling were investigated as a model describing the biological circadian rhythms [48]. In [12] the model of three coupled van der Pol oscillators is applied to the analysis of the problem of synchronous generation of thee coupled vircators (microwave electronics). The dynamics of ring of three phase oscillators was discussed in [49, 50], and networks of four or more coupled oscillators were discussed in [51, 52]. It should be noted, however, that the works, which report the observation of four-frequency quasiperiodicity, are rare. For example, in [53] the authors have presented results of experimental observation of four-frequency oscillations in driven semiconductor system with pn-junctions.

Recently new interesting aspects of the problem of synchronization of two oscillators by external force were revealed in [53-59]. In a series of papers [53-55] mechanisms of synchronization of resonant limit cycles on a torus were established and discussed and they appeared to be different from those of synchronization of the “general case” limit cycle. The corresponding experiment is described in [57]. In [56] phase equations describing the excitation of two coupled self-oscillators by external force were obtained and analyzed. The authors have shown that saddle-node bifurcation of stable and unstable invariant curves solutions of phase equations accounts for appearance of three-frequency oscillations and this corresponds to the similar bifurcation of 2D tori in original system. In [58] the authors analyze the same parameter plane using the method of the charts of Lyapunov exponents. This method revealed a large number of resonant two-frequency quasi-periodic regimes. The authors have also shown that synchronization picture is characterized by two qualitatively different situations. These situations correspond to a regime of mode-locking of two autonomous coupled oscillators and to a regime of their beats.

Synchronization of three coupled oscillators by the external force was discussed in a similar way in [59].

In present work we develop the methods used in Refs. [56-59] for studying the forced coupled oscillators and apply them to the problem of the synchronization phenomena in the chain of coupled phase oscillators. The number of the oscillators in the chain will be increased gradually, so we will observe the quasi-periodic regimes of growing dimension. We will vary the frequency detuning between the second and the first oscillators and coupling parameter to study relative position of the regions of complete synchronization, quasi-periodic regimes and chaos in the parameter plane. Note, that in most works devoted to the chains of oscillators, authors have usually considered the case of a large number of the elements in the chain and specific (for example linear or random) law of variation of the eigen-frequencies of the oscillators in the chain [1, 61, 62]. In this case, the important aspects of the synchronization picture which occurs in the intermediate case (3-5 elements in the chain) are not revealed.

Another issue which we will discuss by the example of a system of three coupled oscillators is what features of synchronization picture will remain valid, when we pass from the system of phase equations to the original system of coupled van der Pol oscillators. It turns out, that there are some nontrivial situations, when the phase approximation is not "working" even for small values of the control parameters. The interesting regime called "broad-band two-frequency synchronization" can be observed in the original system. This regime is due to the special position of the central oscillator sins it is a subject of a greater friction from neighbors. This regime causes a dramatic increase in the range of frequency detuning over which two-frequency synchronization occurs. In other words, two-frequency synchronization can in principle occur for arbitrarily large frequency differences at finite coupling strengths. Moreover, we will show that characteristic sequences of bifurcations, which are typical for phase model and are associated with the possibility of two- and three-frequency quasi-periodicity, may be destroyed. We will also present and discuss the results for the case of the large values of the control parameters as well as for the case of non-identical oscillators.

Part 1. Phase dynamics of the three coupled self-oscillators.

1.1. Phase equations.

Let us consider a system of three dissipatively coupled van der Pol oscillators (Fig.1):

$$\begin{aligned} &\ddot{x} - (\lambda - x^2)\dot{x} + x + \mu(\dot{x} - \dot{y}) = 0, \\ &\ddot{y} - (\lambda - y^2)\dot{y} + (1 + \Delta_1)y + \mu(\dot{y} - \dot{x}) + \mu(\dot{y} - \dot{z}) = 0, \\ &\ddot{z} - (\lambda - z^2)\dot{z} + (1 + \Delta_2)z + \mu(\dot{z} - \dot{y}) = 0. \end{aligned} \qquad (1)$$

Here λ is an excitation parameter in each independent oscillator; Δ_1 and Δ_2 are frequencies detuning between the second and the first oscillators and the third and the first oscillators, respectively; μ is the coupling coefficient. The frequency of the first oscillator is assumed to be normalized by one.

In the case when all parameters in system (1) are small, it may be analyzed in terms of complex amplitudes (quasi-harmonic approximation) [1-3, 8, 9] and we have obtainer the next "truncated equation"

$$
\begin{aligned}
2\dot{a} &= a - |a|^2 a - \mu(a-b),\\
2\dot{b} &= b - |b|^2 b + i\Delta_1 b - \mu_1(b-a) - \mu(b-c).\\
2\dot{c} &= c - |c|^2 c + i\Delta_2 - \mu(c-b).
\end{aligned}
\tag{2}
$$

Here $a(t)$, $b(t)$ and $c(t)$ are the complex amplitudes of the oscillators which are varying slowly in comparison with the basic oscillations with the unit frequency. The parameter λ is eliminated in these equations via a change of the variables and parameters.

Following the Refs. [1-3], we introduce real amplitudes R, r, v and phases $\psi_{1,2,3}$ as $a = \mathrm{Re}^{i\psi_1}$, $b = re^{i\psi_2}$, $c = ve^{i\psi_3}$ and assume that the motion takes place close to the unperturbed limit cycles of the oscillators, i.e. $R = r = v = 1$. Then we obtain the following phase equations:

$$
\begin{aligned}
\dot{\psi}_1 &= \frac{\mu}{2}\sin(\psi_2 - \psi_1),\\
\dot{\psi}_2 &= \frac{\Delta_1}{2} + \frac{\mu}{2}\sin(\psi_1 - \psi_2) + \frac{\mu}{2}\sin(\psi_3 - \psi_2),\\
\dot{\psi}_3 &= \frac{\Delta_2}{2} + \frac{\mu}{2}\sin(\psi_2 - \psi_3).
\end{aligned}
\tag{3}
$$

Let us introduce the relative phases of the oscillators

$$
\theta = \psi_1 - \psi_2, \qquad \varphi = \psi_2 - \psi_3. \tag{4}
$$

Then we rewrite the system (3) in the next form

$$
\begin{aligned}
\dot{\theta} &= -\frac{\Delta_1}{2} - \mu\sin\theta + \frac{\mu}{2}\sin\varphi,\\
\dot{\varphi} &= \frac{\Delta_1 - \Delta_2}{2} - \mu\sin\varphi + \frac{\mu}{2}\sin\theta.
\end{aligned}
\tag{5}
$$

The equations (5) are the phase equations (phase approximation) of the system (1), that we wanted to obtain.

1.2. Complete synchronization of the three oscillators and its destruction.

Complete synchronization is the simple regime in the system (5). It is the regime when the exact phase locking of all oscillators takes place. Phase portrait plotted on the (θ, φ) plane for this case is presented in Fig.2*a*. One can see that the system (5) has four equilibrium points. They are stable and unstable nodes and two saddles. Stable node corresponds to the complete synchronization.

Let us find bifurcations of the equilibrium points of the system (5). For this aim we use the next method. (It is easily generalized to a larger number of oscillators).

The condition of the exact phase locking of all oscillators is $\dot{\psi}_1 = \dot{\psi}_2 = \dot{\psi}_3$. Then $\dot{\theta} = 0$ and $\dot{\varphi} = 0$. In this case the equations (5) may be solved for the sine of phases:

$$
\mu\sin\theta = -\frac{\Delta_1 + \Delta_2}{3}, \qquad \mu\sin\varphi = \frac{\Delta_1 - 2\Delta_2}{3} \tag{6}
$$

If $\sin\theta = \sin\varphi = \pm 1$ then we obtain

$$\mu = \pm\frac{\Delta_1 + \Delta_2}{3}, \tag{7}$$

$$\mu = \pm\frac{\Delta_1 - 2\Delta_2}{3}. \tag{8}$$

We fix one of the frequency detuning, for example Δ_2, and consider organization of the parameter plane (Δ_1, μ). The bifurcation lines given by the conditions (7) and (8) are represented in Fig.3. They define two classical synchronization tongues with the top at the points

$$\Delta_1 = -\Delta_2 \quad \text{and} \quad \Delta_1 = 2\Delta_2. \tag{9}$$

These points are denoted by arrows in Fig.3. The intersection of these tongues gives the region of complete synchronization P. There are four equilibrium points (one stable and three unstable points) of the system (5) in the region P (Fig.2*a*). The stable equilibrium corresponded to the regime then all three oscillators are phase locked.

When we go outside the region P and intersect the left border indicated as SNP_1, four equilibrium points merge in pairs. The phase portrait for this case is shown in Fig.2*b*. After this equilibrium points disappear and one can see stable and unstable invariant curves on the (θ,φ) plane (Fig.2*c*). So, the regime of the complete synchronization is destroyed with an appearance of the two-frequency quasi-periodic oscillations. One can see in Fig.2*c* that the stable invariant curve corresponds to the oscillations of the phase θ near the equilibrium state. Because θ is the relative phase of the first and the second oscillators, it means that the first and the second oscillators are *partially phase locked*. If we intersect the right border of the region P, equilibrium points merge in pairs but in accordance with another rule (Fig.2*d*). As a result, the complete synchronization also destroys. In this case the system (5) demonstrates the two-frequency quasi-periodic regime when the relative phase φ oscillates (Fig.2*e*). It is a regime of the partially phase locking of the second and the third oscillators.

It is easy to see that the destruction of the complete synchronization corresponds to the special type of the bifurcation, when there are two saddle-node bifurcations of the equilibrium points at the same time. Let us explain the mechanism of the observed behavior. One can see from the equations (6), that its solutions appear in pairs. The phases θ_1 and θ_2 are the solutions of the first equation in (6). And the phases φ_1 and φ_2 are the solutions for the second equation in (6). So there are four equilibrium points: (φ_1,θ_1), (φ_1,θ_2), (φ_2,θ_1), (φ_2,θ_2). These points are placed in the vertices of the rectangle on the phase plane. And theirs stable and unstable manifolds organize closed heteroclinic contour (Fig.2*a*). Let us vary one of the combinations of the parameters in (6), for example $\frac{\Delta_1 - 2\Delta_2}{3}$. Then, we obtain, that while θ_1 and θ_2 are constant, φ_1 and φ_2 are moving close to each other. (This is shown by arrows in Fig.2*b*). If the condition (6) is satisfied, the phases φ_1 and φ_2 are merged. After this bifurcation there are two manifolds, from which stable and unstable invariant curves arise.

If we will vary another combination in (6), the solutions θ_1 and θ_2 will merge. As a result, another pair of the manifolds occurs (Fig.2*d*). This situation takes place when we are moving through the right border (SNP_2) of the region P.

The lines SNP_1 and SNP_2 of the saddle-node bifurcations are finished in the common point

$$\mu_c = \frac{\Delta_2}{2}, \quad \Delta_c = \frac{\Delta_2}{2}. \tag{10}$$

We can find this point if we combine the conditions (7) and (8).

In work [13] the same point is called as *saddle node fan*. So we indicated this point as *SNF* in Fig.3. SNF point corresponds to the co-dimension-2 bifurcation. All four equilibrium points are moving towards the one point and disappear there. It means that the region of the complete synchronization has a threshold value of the coupling parameter. It was not observed in the case of two coupled oscillators.

One can see also the saddle-node bifurcation of the invariant curves if we will vary the frequency detuning Δ_1. In such case the stable and unstable invariant curves are moving towards each other, merge and disappear. Two-frequency quasi-periodic regime destroys and the three-frequency quasi-periodic regime arises. Fig.2*f* shows the flow of phase trajectories that corresponds to such three-frequency quasi-periodic regime.

1.3. Different regimes of the three coupled oscillators.

In the previous section we have described the simplest regimes that are observed in the system of three coupled oscillators. Now, let us analyze the parameter plane of the system (5) in more detail using the numerical methods. Following Ref.[33] we use the method of the construction of charts of the Lyapunov exponents. We calculate all Lyapunov exponents Λ_1, Λ_2 of the system (5) at each grid point of the parameter plane (Δ_1, μ). Then we color the points on the plane in accordance with values of the Lyapunov exponents to visualize the domains of the corresponding regimes:

a) *P* is the region of the stable equilibrium point (complete phase locking). The Lyapunov exponents are $\Lambda_1 < 0,\ \Lambda_2 < 0$,

b) T_2 is the region of the two-frequency quasi-periodic regime. The Lyapunov exponents are $\Lambda_1 = 0,\ \Lambda_2 < 0$,

c) T_3 is the region of the three-frequency quasi-periodic regime. The Lyapunov exponents are $\Lambda_1 = 0,\ \Lambda_2 = 0$.

Note that the two-frequency quasi-periodic regime T_2 corresponds to an attractor in the form of the two-frequency torus in the terms of the original system (1). Accordingly, the three-frequency torus corresponds to the three-frequency quasi-periodic regime T_3.

The chart of the Lyapunov exponents plotted using the method which was mentioned above is presented in Fig.4. Firstly, note that the region *P* of the complete phase locking of all oscillators

corresponds to the results of the analytical investigation. The region of the three-frequency quasi-periodic regimes occupies the lower part of the chart. The domains of the two-frequency quasi-periodic regimes look like the synchronization tongues. The tops of these tongues lie on the axis Δ_1.

Different types of the resonant two-frequency regimes correspond to the different tongues. They admit a simple classification. The invariant curves on the "phase square" ($0 < \theta < 2\pi$, $0 < \varphi < 2\pi$) are attractors of the system (5) (Fig.2). These curves can be classified using the factor $w=p:q$. Here p and q are the numbers of crossings of the invariant curve with the sides of the "phase square" [34]. At the same time we must take into account only essential intersections. If the trajectory goes through the upper boundary outside the "phase square" and enters inside it through the lower boundary, then p is increased by one. Otherwise, p is decreased by one. The number q is calculated by similar way.

Because the phase space is 2π-periodic with respect to the variables θ and φ, the phase dynamic may be observed on the torus [34] (see Fig.5). In this case the two-frequency quasi-periodic regimes correspond to the closed attracting orbits on the surface of the torus (Fig.5*a*). The three-frequency quasi-periodic regimes correspond to a trajectory which covers the torus densely (Fig.5*b*). Factor $w=p:q$ is a winding number in this case. It is a rational number for the two-frequency regimes and an irrational number for the three-frequency regimes.

For the more detail description and classification of the observed regimes we add the winding number chart of the two-frequency regimes to the chart of the Lyapuniv exponents [35]. For this we compute values of the numbers p and q in each point on the parameter plane. Then we calculate the winding number $w=p:q$. Thereafter, we color point on the parameter plane in different colors in accordance with the value of number $w=p:q$.

Fig.6 shows the winding number chart plotted for the more interesting fragment of the parameter plane in the neighborhood of the point *SNF*. The winding numbers for the main two-frequency regimes are indicated in Fig.6. The light grey tone designates the three-frequency regimes, which are diagnosed as non-periodic regimes.

The largest tongues of the resonant two-frequency regimes have winding numbers w=0:1 and w=1:0 (Figs. 5 and 6). These tongues correspond to the regimes of the phase locking between the first and the second oscillators (Fig.2c) and between the second and the third oscillators (Fig.2e). One can see also less wide tongues with the winding numbers w=1:2 and w=2:1. In this case phases are infinitely increasing.

As one can conclude from Fig.6*a* the *SNF* point is an important example of the codimention-2 bifurcation in the system with the three-frequency quasi-periodicity. The regimes of the complete synchronization, partial locking between the pairs of oscillators (first-second and second-third) and the three-frequency quasi-periodicity are observed near this point. In turn, there is a set of regions of the two-frequency regimes inside the region of the three-frequency quasi-periodicity. The widest regions correspond to the winding numbers 1:2 and 2:1, 1:3 and 3:1 etc. (Fig.6b). All these regions have the tops at *SNF* point. And the borders of all regions are the lines of saddle-node bifurcation for corresponding

invariant curves.

An existence of these *SNF* points is an important feature of the problem of three-frequency quasi-periodicity. The similar points are discussed in the work [13] for the case of coupled rotation maps (see Fig.4.21 in [13]). The similar points are observed also in the works [31-33] for the problem of the forced synchronization of the two coupled phase oscillators.

Part 2. Dynamic of the three coupled van der Pol oscillators.

2.1. The case of the small value of the control parameters.

In the part 1 we have discussed the dynamics of the system (1) using the phase approximation. Now, let us consider the initial system (1). In this case, the dynamics of the system depends on the value of the parameter λ. Let us consider the case of small values of the parameter λ. Then we may compare results obtained for the phase model (5) with results obtained for the system (1). The chart of the Lyapunov exponents for the system (1) for $\lambda = 0.1$ and $\Delta_2 = 0.05$ is presented in Fig.7*a*. The method of plotting this chart and the color palette are the same as for the phase model.

One can see that the domain of the complete synchronization has the threshold on the coupling parameter. The enlarged fragment of the chart is shown in Fig. 7*a*. It is similar to the case of the phase model (5). At the same time, there are some differences. Let us discuss these differences in more detail.

At first, there is a region of "oscillator death" (*OD*). This is a region where the system (1) has no oscillations because of the large dissipative coupling [1, 19]. This regime is observed when $\mu > \lambda$ (Fig.7*a*). Note, that the line $\mu = \lambda$ is indicated by an arrow in the Fig.7.

The wide band of the two-frequency quasi-periodicity indicated as *PBS* in the parameter range $\lambda/2 < \mu < \lambda$ is another new feature (Fig.7*a*). This regime is possible for arbitrarily large frequency detuning Δ_1. The possibility of an existence of wide band of synchronization regime is known for two dissipatively coupled oscillators [62, 63] and is called broadband synchronization. However, it was observed in the case of unequal control parameters ($\lambda_1 \neq \lambda_2$). In this case in the region of $\lambda_1 < \mu < \lambda_2$ only the first oscillator is significantly suppressed due to the dissipative coupling. As a result, the second oscillator is dominant. So the system of two coupled oscillators demonstrates a regime of the broadband synchronization.

An appearance of the similar features in our case seems to be paradoxical, because all oscillators are identical in control parameters. The reason is that the coupling perturbs differently oscillators in the chain (Fig. 1) even if the control parameters are identical. A qualitative explanation for this effect is presented below.

Let us "turn off" successively in each equation of the system (1) the action from the two other oscillators. Physically, it may be realized if we introduce very large detuning of the frequencies of the oscillators. In this case, we obtain equations for single oscillators with smaller (due to the coupling) effective values of the control parameter λ^*. So we have:

- for the first and the third oscillators control parameter is $\lambda^* = (\lambda - \mu)$,
- for the second oscillator control parameter is $\lambda^* = (\lambda - 2\mu)$.

Thus, the condition that the first and the third oscillators are not damped by the coupling is $\lambda > \mu$. For the second oscillator, this condition is $\lambda > 2\mu$. The specific role of the second oscillator can be easily understood physically. Indeed, the first and the third oscillators are affected by only the one neighbor. The second oscillator is affected by the two neighbors (Fig. 1). That is why the second oscillator is more damped than the first and the third oscillators. This fact is connected with the geometry of the chain. For example, this feature is not observed for the oscillators coupled in the ring.

Thus, in the band $\lambda/2 < \mu < \lambda$ the second oscillator is suppressed and easily locked by one of its neighbors. As result, we observe a regime that can be called a *partial broadband synchronization* (*PBS*).

The presence of "non-identity" associated with the unequal position of the oscillators in the chain may result in that the condition of applicability of the phase approximation is not satisfied even if the control parameter is small. For example, in Fig.7b we present the chart of the Lyapunov exponents for $\lambda = 0.2$ and $\Delta_2 = 0.15$. For this value of detuning Δ_2 the threshold value of the coupling corresponding to the complete synchronization is approximately equal to $\mu = \lambda/2$. It is a value when the first oscillator is fully suppressed by the coupling. Accordingly, the phase approximation (which is based on the approximation of the unperturbed orbit) is no longer applicable. As a consequence, the characteristic shape of the "sharp bend" corresponding to the point *SNF* is not observed. The lower boundary of the synchronization region looks like a smooth line.

In Fig.8a,b we present the bifurcation lines corresponding to Fig.7. Enlarged fragments of a region near the threshold of the complete synchronization are shown in the bottom row of the Fig.8 The enlarged fragment in Fig.8a demonstrates that this region has more complicated structure than the same region in the phase model. The *SNF* point is destroyed. Now the saddle-node bifurcations of the stable and unstable regimes do not occur simultaneously. They have their own bifurcation lines. Threshold of the complete synchronization has the form of a smooth line, not a tip. The cusp point of the unstable regimes lies in the vicinity of destroyed *SNF* point. Three unstable limit cycles merge together in this cusp point. In Fig.8b one can see that saddle-node bifurcation curve with an increasing of the amplitude of the force is replaced by Neimark-Sacker bifurcation curve. The Neimark-Sacker bifurcation curve ends at the point of the resonance 1:1. This is similar to the case of the classical synchronization [4]. The boundary of the region of the complete synchronization becomes smoother in Fig.8b. In addition, the cusp point of unstable cycles is located already so far away that we can not longer talk about the picture, which is characteristic for the *SNF* point.

2.2. The case of the large values of the control parameters.

The case when the control parameter value is small was discussed above. Now let us consider the case when it is comparable with the unity. So the phase approximation is obviously inefficient. In addition,

we consider for generality the situation when the control parameters of the oscillators are not equal:

$$\begin{aligned}
&\ddot{x} - (\lambda_1 - x^2)\dot{x} + x + \mu(\dot{x} - \dot{y}) = 0,\\
&\ddot{y} - (\lambda_2 - y^2)\dot{y} + (1+\Delta_1)y + \mu(\dot{y} - \dot{x}) + \mu(\dot{y} - \dot{z}) = 0,\\
&\ddot{z} - (\lambda_3 - z^2)\dot{z} + (1+\Delta_2)z + \mu(\dot{z} - \dot{y}) = 0.
\end{aligned} \qquad (11)$$

The chart of the Lyapunov exponents and typical phase portraits of the system (11) are given in Fig.9. They are plotted for $\lambda_1 = 1.3$, $\lambda_2 = 1.9$, $\lambda_3 = 1.8$, $\Delta_2 = 1.5$. In this case, there is no leading oscillator inside the main tongue of the complete synchronization. Oscillators have orbits with approximately equal size (Fig.9a). However, the phase portraits are different from circles. It may be associated with the deviation from the quasi-harmonic approximation.

With the increasing of the coupling parameter μ all oscillators are suppressed one by one. It is seen also in the organization of the parameter plane. In our case parameters obey $\lambda_2/2 < \lambda_1 < \lambda_3$. The central, i.e. the second, oscillator is damped firstly. Then the first oscillator is damped. And only then the third oscillator is damped. Consequently there are two types of broadband synchronization in Fig.9:

- *complete broadband synchronization CBS at* $\lambda_1 < \mu < \lambda_3$,
- *partial broadband synchronization PBS at* $\lambda_2/2 < \mu < \lambda_1$.

The corresponding boundary values of coupling parameter are indicated by arrows in Fig.9.

In the first case, all three oscillators are phase locked. A typical regime of broadband synchronization occurs due to the dominance of the least excited third oscillator. Other oscillators are suppressed by the coupling. Accordingly, the sizes of the limit cycles of the first and the second oscillators are approximately equal, but much less than the size of the limit cycle of the third oscillator (Fig.9b). (See the scales on the axes in the phase portraits.)

In turn, in the band $\lambda_2/2 < \mu < \lambda_1$ only the second oscillator is suppressed by the coupling. In this case, it is easily phase locked by the first oscillator, which is more excited. As a result, the regime of the *partial broadband synchronization* occurs. It corresponds to the two-frequency quasi-periodicity.

The most significant changes occur in the region of the three-frequency quasi-periodicity. New tongues of the two-frequency regimes appear inside it. Phase portraits of the oscillators for the two most typical tongues are presented in Fig.9c,d. In this case, the damping effect is negligible for all three oscillators. Now the central oscillator is dominant, because it has the largest value of the control parameter $\lambda_2 > \lambda_3 > \lambda_1$. At the same time, inside each of these two tongues there is an oscillator, which is mostly quasi-periodically perturbed - it is the third oscillator in Fig.9c and the first oscillator in Fig.9d. It corresponds to the fact that the first and the second oscillators are phase locked in the first case, and the second and the third oscillators are phase locked in the second case.

This fact may be explained by introducing the rotation numbers of the oscillators relative to each other. For this we choose the Poincare section for each oscillator. The conditions for the Poincare sections are $\dot{x} = 0$, $\dot{y} = 0$ and $\dot{z} = 0$ for the first, the second and the third oscillators, correspondingly. We calculate

the number of returnings of the phase trajectory in each section N_x, N_y, N_z for a long period of time. Then we define the rotation number of the first oscillator in relation to the second one as $\nu_{1-2} = \frac{N_x}{N_y}$ and the rotation number of the second oscillator in relation to the third one as $\nu_{2-3} = \frac{N_y}{N_z}$. (These rotation numbers are not the same as the factor *w* introduced in the section 1.3. The quantity *w* characterizes the relative positions of the three main spectral components in a small neighborhood of the central frequency of the oscillators, i.e. $\Delta \approx 0$ in our case in Fig.9.)

Fig.10 shows the rotation numbers ν_{1-2} and ν_{2-3} as the function of the frequency detuning Δ_1 for a fixed level of the coupling. This level of the coupling is indicated by the white dotted line in Fig.9. One can see the typical plateaus at $\nu_{1-2} = 1:3$ and $\nu_{2-3} = 3:1$. Thus, in this case, we observe multiple synchronization of the oscillators with a ratio of 1:3 of the main spectral components. Although the two-frequency torus is a phase portrait of the system, these regimes have no analogue in the phase approximation. It can be assumed that the boundaries of the corresponded tongues of the two-frequency regimes in Fig.9 are the lines of the saddle-node bifurcations. (At least in the case of small values of the coupling.)

Part 3. Phase dynamics of the four phase oscillators.

3.1. Phase equations and a condition of the complete synchronization.

Let us increase the number of the oscillators and consider the chain of the four dissipatively coupled van der Pol oscillators:

$$\begin{aligned}
&\ddot{x} - (\lambda - x^2)\dot{x} + x + \mu(\dot{x} - \dot{y}) = 0,\\
&\ddot{y} - (\lambda - y^2)\dot{y} + (1+\Delta_1)y + \mu(\dot{y} - \dot{x}) + \mu(\dot{y} - \dot{z}) = 0,\\
&\ddot{z} - (\lambda - z^2)\dot{z} + (1+\Delta_2)z + \mu(\dot{z} - \dot{y}) + \mu(\dot{z} - \dot{w}) = 0,\\
&\ddot{w} - (\lambda - w^2)\dot{w} + (1+\Delta_3)w + \mu(\dot{w} - \dot{z}) = 0.
\end{aligned} \tag{12}$$

Following the section 1.1, we obtain the equations for the phases of oscillators:

$$\begin{aligned}
\dot{\theta} &= -\frac{\Delta_1}{2} - \mu\sin\theta + \frac{\mu}{2}\sin\varphi,\\
\dot{\varphi} &= \frac{\Delta_1 - \Delta_2}{2} + \frac{\mu}{2}\sin\theta - \mu\sin\varphi + \frac{\mu}{2}\sin\phi,\\
\dot{\phi} &= \frac{\Delta_2 - \Delta_3}{2} + \frac{\mu}{2}\sin\varphi - \mu\sin\phi.
\end{aligned} \tag{13}$$

Here we use the relative phases of the oscillators:

$$\theta = \psi_1 - \psi_2, \quad \varphi = \psi_2 - \psi_3. \quad \phi = \psi_3 - \psi_4. \tag{14}$$

Let us find the conditions for the complete synchronization of the system (13), for which we set $\dot{\theta} = \dot{\varphi} = \dot{\phi} = 0$. Then we obtain the following equations from (13):

$$\mu \sin\theta = -\frac{\Delta_1 + \Delta_2 + \Delta_3}{4},$$
$$\mu \sin\varphi = \frac{\Delta_1 - \Delta_2 - \Delta_3}{2}, \qquad (15)$$
$$\mu \sin\phi = \frac{\Delta_1 + \Delta_2 - 3\Delta_3}{4}.$$

There are eight equilibrium points located at the corners of the box in the phase space (θ,φ,ϕ), provided all equations in (15) have solutions. Two of the box faces can move closer with the variation of any combinations of the parameters in the right side of (15). As a result, all eight equilibrium points merge in pair and simultaneously disappear as soon as one of the values of the sine function of the phase variables is becomes equal to ± 1. The picture is similar to the phase system (5), but it is embedded in the three-dimensional phase space. Assuming each sine of the phase variables in (13) equal to ± 1, we obtain the following conditions:

$$\mu = \pm\frac{\Delta_1 + \Delta_2 + \Delta_3}{4}, \qquad (16)$$

$$\mu = \pm\frac{\Delta_1 - \Delta_2 - \Delta_3}{2}, \qquad (17)$$

$$\mu = \pm\frac{\Delta_1 + \Delta_2 - 3\Delta_3}{4}. \qquad (18)$$

The relations (16-18) determine the three tongues in the parameter plane (Δ_1,μ). The tops of these tongues are at

$$\Delta_1 = -\Delta_2 - \Delta_3,$$
$$\Delta_1 = \Delta_2 + \Delta_3, \qquad (19)$$
$$\Delta_1 = -\Delta_2 + 3\Delta_3.$$

Now we shall discuss the saddle-node bifurcations of equilibrium points, which are responsible for the destruction of the complete synchronization. As in the case of three coupled oscillators, we use the parameter plane (Δ_1,μ) and the relations (16-18). The conditions (16) and (18) define the four lines in this plane (Fig.11). The center of two symmetrical tongues in Fig.11a corresponds to the point with coordinates $\Delta_1 = -\Delta_2 + \Delta_3$ and $\mu = \Delta_3/2$. As in the case of three coupled oscillators, both tongues do not correspond to the equilibrium regimes at small coupling. However, now even the overlapping of these two tongues, which is shown in Fig.11a by the light gray color, may not correspond to the stable equilibrium regimes. It depends on the position of the third tongue (17).

In order to classify the regimes of the system (13) we follow the relative position of the tongue (17) and the region shown in the light gray color in Fig.11. The ordinates of their tops are $\Delta_1 = -\Delta_2 + \Delta_3$ and $\Delta_1 = \Delta_2 + \Delta_3$, respectively. Let us consider the change of the relative position of these regions with the decreasing of the frequency mismatch Δ_2. Fig.11a shows the configuration occurring when the condition

$\Delta_2 > \frac{\Delta_3}{2}$ is valid. The corresponding region of the complete synchronization of all four oscillators is shown by the dark gray color (red color on-line). The regime of complete synchronization has in this case the threshold value in the coupling parameter. We find it by combining the relations (16) and (18):

$$\mu_c = \frac{\Delta_3 + \Delta_2}{3}, \quad \Delta_c = \frac{\Delta_3 + \Delta_2}{3}. \tag{20}$$

The tongues in Fig.11a move closer one by one with a decreasing of the frequency detuning Δ_2. The point of intersection of tongues boundaries moves to another branch when $\Delta_2 < \frac{\Delta_3}{2}$. And the situation shown in Fig.11b takes place. The form of the region of the complete synchronization of the four coupled oscillators changes in this case. And the threshold value of coupling depends no longer on Δ_2. It corresponds to the value

$$\mu_c = \frac{\Delta_3}{2}, \quad \Delta_c = \Delta_3 - \Delta_2. \tag{21}$$

Then the situation is repeated symmetrically. Thus, there are two possible types of the region of the complete synchronization of four coupled oscillators. They are shown in Fig.11a and b.

3.2. Different regimes of the system of four coupled oscillators.

Now let us discuss the organization of the parameter space of four coupled oscillators in detail. Fig.12a shows a chart of the Lyapunov exponents of the system (13) on the parameter plane (Δ_1, μ). The system (13) is characterized already by the three Lyapunov exponents. Hence, the regimes of the four-frequency quasi-periodicity and chaos are now possible. Areas of different regimes in Fig.12a are marked as follows:

a) *P* is the region of the stable equilibrium point (i.e. the complete phase locking). The Lyapunov exponents are $\Lambda_1 < 0,\ \Lambda_2 < 0,\ \Lambda_3 < 0$,

b) T_2 is the region of the two-frequency quasi-periodic regime. The Lyapunov exponents are $\Lambda_1 = 0,\ \Lambda_2 < 0,\ \Lambda_3 < 0$,

c) T_3 is the region of the three-frequency quasi-periodic regime. The Lyapunov exponents are $\Lambda_1 = 0,\ \Lambda_2 = 0,\ \Lambda_3 < 0$,

d) T_4 is the region of the four-frequency quasi-periodic regime. The Lyapunov exponents are $\Lambda_1 = 0,\ \Lambda_2 = 0,\ \Lambda_3 = 0$,

e) C is the region of chaos. The Lyapunov exponents are $\Lambda_1 > 0,\ \Lambda_2 < 0,\ \Lambda_3 < 0$.

The values of other parameters are chosen as Δ_1=0.3 and Δ_2=1. In this case we have the most complex configuration of a region of the complete synchronization (Fig.11b).

In Fig.12a one can see the region of the complete synchronization *P*. It corresponds to the results of

an analytical review presented in Fig.11b. The region of the complete synchronization adjoins the domains of the two-frequency regimes, except the points 1, 2, and 3 indicated by arrows. In these points the region of the complete synchronization has a "point" contacting with the region of the three-frequency quasi-periodicity.

The tops of the tongues of two-frequency regimes on the axis of frequency detuning parameter are destroyed. It is unlike the case of three coupled oscillators (compare Fig.12 and Fig.4). The region of the two-frequency quasi-periodicity is surrounded by the region of the three-frequency regimes located mostly above the line $\mu \approx 0.3$. The four-frequency quasi-periodicity is dominant at lower values of coupling. However, there are two tongues of the three-frequency regimes at very small values of coupling. The tops of these tongues are located on the frequency axis. There are also the regions of chaos for the system of four coupled oscillators. But these regions are very small and are located on the border of the three- and four-frequency regimes.

The chart of the winding numbers is added to the chart of the Lyapunov exponents (Fig.12b). The regions of different two-frequency resonant regimes are shown on this chart by different colors. The two-frequency regimes are indicated by the winding numbers $w = p:q:r$. Here p, q and r correspond to the numbers of significant intersections of the invariant curve with the sides of the phase cube in the space of the relative phases of oscillators (θ, φ, ϕ).

3.3. Co-dimension-2 and -3 situations.

There are three points of co-dimension-2 marked by the numbers 1, 2 and 3 on the Fig.12a. The pairs of different lines of the saddle-node bifurcations of equilibrium points are converged at these points. The enlarged fragments of Fig.12b in the vicinity of the points 1 and 2 are shown in Fig.13.

Firstly, we consider a neighborhood of the point marked in Fig.12a by the number 1 (Fig.13a). Its structure is similar to the structure of a neighborhood of *SNF* point. Indeed, all winding numbers have the form $w = 0:q:r$. It means that the first and the second oscillators are partially locking. (Their relative phase oscillates with the limited amplitude and does not increase. Zero index in the winding number corresponds to this fact.) The system (13) is clustered as shown in Fig.14a. And the remaining two indices $q:r$ are similar to the winding number in the case of three coupled oscillators (see Fig.6). Thus, the dynamics of the system (13) is similar to the case of three coupled oscillators. And the sub-system consists from the first and the second partially locked oscillators.

It is easy to see from Fig.13*b* that a similar situation occurs in the neighborhood of the second *SNF* point. The second and the third oscillators are partially locked in this case. It is shown schematically in Fig.14b. In this case the winding numbers are in the form of $w = p:0:r$.

A similar situation occurs also in the neighborhood of the third point of intersection of the saddle-node bifurcations. One can see from Fig.12b that the winding numbers in this case are in the form $w = p:q:0$. It corresponds to the situation when the third and the fourth oscillators are partially locked

(Fig.14c). However, the form of the regions is not typical for the *SNF* point. Indeed, the presence of the regions with the winding numbers $p:q=1:0$ and $p:q=0:1$ is characteristic to this point in its small neighborhood. However, these regions are separated from the point 3 in Fig.12c. Correspondingly, the location of the regions of the resonant regimes with the winding numbers 2:1:0, 3:2:0, 4:3:0, etc. looks differently.[1]

Let us return to Fig.11. It is easy to see that via tuning the frequency mismatch Δ_2 we can achieve a situation when two "corners" on Fig.11b merge. Thus, a new *situation of co-dimension*-3 takes place. In this case all three lines (16-18) are intersecting at one point. We can easily obtain the condition of realization of this co-dimension-3 bifurcation by the combining the relevant equations. It is $\Delta_2 = \frac{\Delta_3}{2}$.

The situation before the threshold of this bifurcation corresponds to the two points of SNF type (Fig.13a). Thus, this bifurcation can be interpreted as a mergence of two such points.

Fig.15 shows the chart of the winding numbers at the point of such bifurcation. One can see that the SNF type points are destroyed. Now the regions of different types converge at one point. These regions correspond to a partial locking of the first and the second oscillators ($w=0:q:r$) and also to a partial locking of the second and the third oscillators ($w=p:0:r$). However, these two groups are clearly separated by the tongue with the winding number $w=0:0:1$. This tongue corresponds to the partial locking of the three oscillators. They are the first, the second and the third oscillators.

Beyond the threshold of bifurcation when $\Delta_2 > \Delta_3/2$, the set of tongues with the winding numbers $w=p:q:0$ occurs between the regions $0:1:0$ and $1:0:0$. These tongues correspond to a partial locking of the third and the fourth oscillators. Thus, all the three variants of clustering are presented in the vicinity of the codimension-3 point, each type of clustering corresponds to the phase locking of one of the pairs of oscillators.

Part 4. On the road towards multidimensional tori.

The discussed above method of the analysis of the phase equations can be extended to the case of the larger number of oscillators. For example, for the five coupled oscillators we have the following equations instead of equations:

$$\begin{aligned}
\dot{\theta} &= -\frac{\Delta_1}{2} - \mu\sin\theta + \frac{\mu}{2}\sin\varphi, \\
\dot{\varphi} &= \frac{\Delta_1 - \Delta_2}{2} + \frac{\mu}{2}\sin\theta - \mu\sin\varphi + \frac{\mu}{2}\sin\phi, \\
\dot{\phi} &= \frac{\Delta_2 - \Delta_3}{2} + \frac{\mu}{2}\sin\varphi - \mu\sin\phi + \frac{\mu}{2}\sin\vartheta, \\
\dot{\vartheta} &= \frac{\Delta_3 - \Delta_4}{2} + \frac{\mu}{2}\sin\phi - \mu\sin\vartheta.
\end{aligned} \tag{22}$$

[1] Note that the presented discussion is based on visual estimates of the form of the charts obtained numerically. The detailed bifurcation analysis of the two-frequency quasi-periodic regimes is necessary for a more strict justification and identifying picture details.

Let us set $\dot{\theta} = \dot{\varphi} = \dot{\phi} = \dot{\vartheta} = 0$ for the equilibrium points searching. We use the algorithm described above. We express $\sin\varphi$ through $\sin\theta$ in the first equation and substitute it into the second equation. Then we express $\sin\phi$ through $\sin\theta$ in the second equation, and so on. As a result, we obtain the following expressions for the sine of the four phase variables:

$$\begin{aligned}
\mu\sin\theta &= -\frac{\Delta_1 + \Delta_2 + \Delta_3 + \Delta_4}{5}, \\
\mu\sin\varphi &= \frac{3\Delta_1 - 2\Delta_2 - 2\Delta_3 - 2\Delta_4}{2}, \\
\mu\sin\phi &= \frac{2\Delta_1 + 2\Delta_2 - 3\Delta_3 - 3\Delta_4}{5}, \\
\mu\sin\vartheta &= \frac{\Delta_1 + \Delta_2 + \Delta_3 - 4\Delta_4}{5}.
\end{aligned} \tag{23}$$

This system has 16 equilibrium points at the vertices of a four-dimensional parallelepiped in the four-dimensional phase space $(\theta, \varphi, \phi, \vartheta)$ if all the equations (23) have solutions. Similarly to the case of three or four coupled oscillators, the three-dimensional faces of this parallelepiped may move close one to another with the variation of the parameter combination in (23). As a result, the saddle-node bifurcation takes place and all 16 points are merging in pairs and simultaneously disappear.

The condition $\sin\theta = \sin\varphi = \sin\phi = \sin\vartheta = \pm 1$ leads to the following relations:

$$\begin{aligned}
\mu &= \pm\frac{\Delta_1 + \Delta_2 + \Delta_3 + \Delta_4}{5}, \\
\mu &= \pm\frac{3\Delta_1 - 2\Delta_2 - 2\Delta_3 - 2\Delta_4}{2}, \\
\mu &= \pm\frac{2\Delta_1 + 2\Delta_2 - 3\Delta_3 - 3\Delta_4}{5}, \\
\mu &= \pm\frac{\Delta_1 + \Delta_2 + \Delta_3 - 4\Delta_4}{5}.
\end{aligned} \tag{24}$$

Now there are four tongues on the plane (Δ_1, μ). Two tongues have the same smaller slope 1/5. And two tongues have greater slopes (2/5 and 3/5). It is easy to show that the region of intersection of these tongues may have no more than four "corners". These “corners” correspond to the co-dimension-2 points. Fig.16 shows a qualitative picture that illustrates the corresponding configuration.

The presence of this configuration can be explained as follows. Organization of the parameter plane obtained by means of the first and the fourth lines from (24) and supplemented by the third line from (24) is similar to the case of three coupled oscillators. It follows from (24) that this region has three "corners", when the condition $\Delta_3 < \frac{\Delta_4}{2}$ is satisfied. In this case the region of complete synchronization has a threshold in the coupling parameter. It is determined by the relations

$$\mu_c = \frac{\Delta_4}{2}, \qquad \Delta_c = \frac{3}{2}\Delta_4 - \Delta_3 - \Delta_2. \tag{25}$$

This picture must be supplemented by two lines which define the second tongue (24) (Fig.16). And if

this tongue includes the point (25), this point determines the threshold of a region of the complete synchronization.

As an illustration, in Fig.17 we present a Lyapunov exponents chart for the case of five oscillators. In this case, a region of five-frequency quasiperiodicity T_5 arises, which is shown in Figure 17 in green. For large values of the frequency parameter Δ_1 (the right edge of the Fig.17a) the cascade of saddle-node bifurcations of quasi-periodic regimes with successively increasing dimension can be observed. Enlarged fragment of the chart in Fig. 17b illustrates the emergence of chaos at intermediate values of the coupling parameter. You can also see a system of fan-shaped two-frequency resonant tongues.

It is easy to see that in addition to the codimension-2 and -3 situations, described in the previous paragraph, we can achieve a situation of higher co-dimension-4 by varying the required number of parameters. In this case three points of co-dimension-2 are merging. It takes place under the following condition

$$\Delta_2 = \frac{\Delta_4}{5}, \ \Delta_3 = \frac{\Delta_4}{2}. \tag{26}$$

And the coordinates of corresponding point on the plane (Δ_1, μ) are

$$\mu = \frac{\Delta_4}{2}, \ \Delta_1 = \frac{4\Delta_4}{5}. \tag{27}$$

The discussed results may be generalized to any number of the coupled oscillators. If we have (N +1) coupled oscillators, then there are N tongues on the parameter plane of frequency detuning and coupling. The region of the complete synchronization is obtained as the overlap of all these tongues. One can see here an analogy with the well-known interpretation of the synchronization of chaos. It follows from this interpretation that synchronization of chaos is due to an intersection of the synchronization tongues of the unstable periodic orbits built into the chaotic attractor [1]. The difference is that in the case of multi-frequency synchronization the number of tongues is finite and less than the number of coupled oscillators by one. And there are certain rules of calculating the tops of the tongues and their boundaries.

The boundary of the region of the complete synchronization is formed by lines of the saddle-node bifurcations. All 2^N equilibrium points are merging in pairs at these lines. This boundary has "corners". They are co-dimension-2 points. The curves of the saddle-node bifurcations of equilibrium states of different types are meeting in these points. At the same time the regime when all oscillators are not phase locked is observed in the regions of small coupling.

Conclusion.

The ensembles of a small number (three to five) of oscillators demonstrate complex behavior, characterized by the coexistence of domains of full synchronization, quasiperiodicity of different dimension, and chaos. We present here a two-parameter picture corresponding to the plane of the frequency detuning parameter and the coupling parameter. To do this, Lyapunov's exponents charts, were constructed, visualizing the domains of quasi-periodicity of different dimensions, illustrating their relative

positions. This method is effective for the analysis of such systems and accessible for modern computers, because the bifurcation analysis of quasi-periodic regime is too complex.

In the system of three coupled phase oscillators the region of the complete synchronization has a threshold value of coupling parameter. This threshold is associated with a co-dimension-2 point. The regions of complete synchronization, of pairwise partial synchronization and of the three-frequency quasi-periodicity are merging at this point. The region of the three-frequency quasi-periodicity involves the system of the tongues of the two-frequency resonant regimes. These regimes can be classified using the rational winding numbers. In the phase space there is a heteroclinic contour in the vicinity of this point. Its destruction is responsible for the occurring of two-frequency quasi-periodicity. The contour shrinks to a point directly at the co-dimension-2 point (*SNF*). These points are typical and important for the phase systems demonstrating three-frequency quasi-periodicity.

Additional features are revealing when we return from phase equations to the original system of differential equations. In the range of values $\lambda/2 < \mu < \lambda$ the second oscillator in the chain is suppressed by the coupling. As result, we observe a regime that can be called two-frequency broadband synchronization. In this case, the second oscillator is partially locked by its neighbors. And the phase locking is possible for an arbitrarily large frequency detuning. The possibility of this effect, which was established earlier for non-identical systems, is associated with the selected position of the central oscillator. It is subjected to twofold friction from its two neighbors.

Mutual arrangement of bifurcation curves responsible for the destruction of complete synchronization changes significantly compared to the phase equation case. *SNP* lines typical for the phase equations are splitting into two lines now. The first line corresponds to the saddle-node bifurcation of stable cycle. The second line corresponds to the saddle-node bifurcation of unstable saddle cycles. The co-dimension-2 bifurcation point typical for phase equations is destroyed too. Two different *SNP* lines are converging to this point. The cusp point arises at the borderline of existence of unstable cycles in the corresponding region.

In the initial system of three coupled van der Pol oscillators new tongues of the two-frequency tori arise in the region of the three-frequency quasi-periodicity for the large values of control parameters. They correspond to the phase locking of the pairs of the oscillators with following ratios of the eigen-frequencies: 1:3, 1:5, etc. In a system with non-identical parameters complete broadband synchronization is possible in the region, where coupling suppresses two oscillators.

In a system of four coupled phase oscillators the region of the complete synchronization also borders the region of the two-frequency regimes except for selected points at which it has a "point" contact with the region of the three-frequency quasi-periodicity. These points correspond to the intersection of two lines of saddle-node bifurcation of equilibrium states of different types. Their neighborhoods may demonstrate three types of clustering in the system, with one pair of oscillators partially locked. Last system is to some extent similar to a chain of three oscillators. However, there are some differences in the regions of the two-

frequency regimes in the case of strong coupling.

These differences are most significant near the co-dimension-3 point, which correspond to the intersection of three lines of the saddle-node bifurcation of equilibrium states. This region is the most representative concerning the variety of types of the observed regimes. In its neighborhood, at the same time, there are three types of clustering, corresponding to the phase locking of the one of the pairs of oscillators. In addition, there are tongues of two-frequency tori that do not correspond to clustered states. These tongues are immersed in the region of chaos. The chaos transforms into the four-frequency quasi-periodic regimes with the decreasing of the coupling parameter.

In the case of four coupled phase oscillators the four-frequency quasi-periodic regimes are dominating. However, there are two narrow tongues of the three-frequency quasi-periodic regimes in the region of very small coupling.

The above described algorithm of searching for the domain of complete synchronization in the chain of phase equations can easily be extended to the case of a larger number of phase oscillators. The specific type of the saddle-node bifurcation accounts for the destroying of the regime of complete synchronization. At the points of this bifurcation curve all the equilibrium points existing in the system are merging pairwise and annihilate simultaneously. *N* conditions define *N* tongues in the parameter plane (frequency detuning – coupling parameter). Region of the complete synchronization corresponds to the domain of overlap of all tongues.

The work supported by the RFBI (grant 11-02-91334) and DFG (grant N220/14-1).
Department of Electronics and Instrumentation, Saratov State Technical University.
Kotel'nikov's Institute of Radio-Engineering and Electronics of RAS, Saratov Branch.

Reference.

1. Pikovsky A., Rosenblum M., Kurths J. Synchronization. Cambridge, 2001, 411 p.
2. Blekhman I., Synchronization of Dynamical Systems, Nauka, Moscow, 1971, 351 p. (in Russian).
3. Balanov A.G., Janson N.B., Postnov D.E., Sosnovtseva O. Synchronization: from simple to complex. Springer, 2009, 437 p.
4. Guckenheimer J. and Holmes P. Nonlinear Oscillations, Dynamical Systems and Bifurcations of Vector Fields, Springer, New York, 1983.
5. Encyclopedia of dynamical systems, http://www.scholarpedia.org.
6. Kuramoto Y. Chemical Oscillations, Waves, and Turbulence. New York: Springer-Verlag, 2003, 148 p.
7. Glass L., MacKey M.C. From Clocks to Chaos. The Rhythms of Life. Princeton University Press, 1988, 248 p.
8. Winfree A. The Geometry of Biological Time. New York: Springer-Verlag, second edition, 2001, 781 p.
9. Mosekilde E., Maistrenko Y., Postnov D. Chaotic Synchronization. Applications to Living Systems. World Scientific Series on Nonlinear Science, Series A, 2002, 440 p.

10. Yu P., Gumel A.B. Bifurcation and stability analyses for a coupled Brusselator model // Journal of Sound and Vibration, 2001, vol. 244, No. 5, p. 795-820.
11. Volkov E.I., Romanov V.A. Bifurcations in the system of two identical diffusively coupled Brusselators // Physica Scripta, 1995, vol. 51, No. 1, p. 19-28.
12. Repin B.G., Dubinov A.E. Phasing of three vircators simulated in terms of coupled van der Pol oscillators // Technical Physics, 2006, vol. 51, No. 4, p. 489-494.
13. Kawahara T. Coupled Van der Pol oscillators - A model of excitatory and inhibitory neural interactions // Biological Cybernetics, 1980, vol. 39, No. 1, p. 37-43.
14. Crowley M.F, Epstein I.R. Experimental and theoretical studies of a coupled chemical oscillator: phase death, multistability and in-phase and out-of-phase entrainment // J. Phys. Chem., 1989, vol. 93, No. 6, p. 2496–2502.
15. Anishchenko V.S., Astakhov V.V., Neiman A.B., Vadivasova T.E., Schimansky-Geier L. Nonlinear Dynamics of Chaotic and Stochastic Systems. Tutorial and Modern Development. Springer, Berlin, Heidelberg, 2007, 460 p.
16. Anishchenko V.S. Dynamical Chaos – Models and Experiments. Appearance Routes and Structure of Chaos in Simple Dynamical Systems. World Scientific Series on Nonlinear Science. Series A, 1995, vol. 8, 384 p.
17. Dmitriev A.S., Kislov V.Y. Stochastic oscillations in radiophysics and electronics, Nauka, Moscow, 1989, 280 p. (in Russian).
18. Madan R. Chua's circuit: A paradigm for chaos, World Scientific, 1993, 1042 p.
19. Aronson D.G., Ermentrout G.B., Kopell N. Amplitude response of coupled oscillators // Physica D, 1990, vol. 41, p. 403-449.
20. Reddy R.D.V., Sen A., Johnston G.L. Experimental evidence of time-delay-induced death in coupled limit-cycle oscillators // Phys. Rev. Lett., 2000, vol.85, p. 3381-3384.
21. Herrero M., Figueras M., Rius J., Pi F., Orriols G. Experimental Observation of the amplitude Death effect in two coupled nonlinear oscillators. // Phys. Rev. Lett. 2000, vol. 84, p. 5312-5315.
22. Bar-Eli K. On the stability of coupled chemical oscillators // Physica D, 1985, vol.14, p. 242-252.
23. Zhai Y., Kiss I.Z., Hudson J.L. Amplitude death through a Hopf bifurcation in coupled electrochemical oscillators: experiments and simulations // Phys. Rev. E, 2004, vol. 69, 026208.
24. Ozden I., Venkataramani S., Long M.A., Connors B.W., Nurmikko A.V. Strong coupling of nonlinear electronic and biological oscillators: reaching the “amplitude death” regime // Phys. Rev. Lett., 2004, vol.93, 158102.
25. Rand R., Holmes P.J. Bifurcation of periodic motions in two weakly coupled van der Pol oscillators // Int. J. Non-Linear Mechanics, 1980, vol. 15, p. 387.
26. Ivanchenko M.V., Osipov G.V., Shalfeev V.D., Kurths J. Synchronization of two non-scalar-coupled limit-cycle oscillators // Physica D, 2004, vol. 189, No. 1-2, p. 8-30.
27. Kuznetsov A.P., Stankevich N.V., Turukina L.V. Coupled van der Pol–Duffing oscillators: Phase

dynamics and structure of synchronization tongues // Physica D, 2009, vol. 238, p. 1203-1215.

28. Storti D.W., Rand R.H. Dynamics of two strongly coupled van der Pol oscillators // Int. J. Non-Linear Mechanics. 1982, vol. 17, No. 3, p. 143-152.
29. Chakraborty T., Rand R.H. The transition from phase locking to drift in a system of two weakly coupled van der Pol oscillators // Int. J. Non-Linear Mechanics, 1988, vol. 23, No. 5/6, p. 369-376.
30. Pastor I., Perez-Garcia V.M., Encinas-Sanz F., Guerra J.M. Ordered and chaotic behavior of two coupled van der Pol oscillators // Phys. Rev. E, 1993, vol. 48, p. 171-182.
31. Poliashenko M., McKay S.R., Smith C.W. Hysteresis of synchronous – asynchronous regimes in a system of two coupled oscillators. // Phys. Rev. A, 1991, vol. 43, p. 5638-5641.
32. Pastor-Díaz I., López-Fraguas A. Dynamics of two coupled van der Pol oscillators // Phys. Rev. E, 1995, vol. 52, No. 2, p. 1480–1489.
33. Poliashenko M., McKay S.R., Smith C.W. Chaos and nonisochronism in weakly coupled nonlinear oscillators // Phys. Rev. A, 1991, vol. 44, p. 3452-3456.
34. Rajasekar S., Murali K. Resonance behavior and jump phenomenon in a two coupled Duffing–van der Pol oscillators // Chaos, Solitons & Fractals, 2004, vol. 19, No. 4, p. 925-934.
35. Pikovsky A., Rosenblum M. Self-organized partially synchronous dynamics in populations of nonlinearly coupled oscillators Physica D, 2009, vol. 238, p. 27-37.
36. Reddy D. V. R., Sen A., Johnston G. L. Time delay effects on coupled limit cycle oscillators at Hopf bifurcation // Physica D, 1999, vol. 129, p. 15-34.
37. Wirkus S. The Dynamics of Two Coupled van der Pol Oscillators with Delay Coupling // Nonlinear Dynamics, 2002, vol. 3, No. 3, p. 205-221.
38. Camacho E., Rand R., Howland H. Dynamics of two van der Pol oscillators coupled via a bath // International Journal of Solids and Structures, 2004, vol. 41, No. 8, p. 2133-2143.
39. Astakhov V.V., Vadivasova T.E, Koblyansky S.A. Anishchenko V.S. Bifurcation analysis of the dynamics of dissipative connected Van der Pol generators // Successes of modern electronics, 2008, No. 9, p. 61-68 (in Russian).
40. Baesens C, Guckenheimer J., Kim S., MacKay R.S. Three coupled oscillators: mode locking, global bifurcations and toroidal chaos // Physica D, 1991, vol. 49, p. 387-475.
41. Linsay P.S., Cumming A.W. Three-frequency quasiperiodicity, phase locking, and the onset of chaos. // Physica D, 1989, vol. 40, p.196-217.
42. Battelino P.M. Persistence of three-frequency quasiperiodicity under large perturbations // Phys. Rev. A, 1988, vol. 38, p. 1495–1502.
43. Ashwin P, Guasch J., Phelps J.M. Rotation sets and phase-locking in an electronic three oscillator system // Physica D, 1993, vol. 66, p. 392-411.
44. Ashwin P, King G. P., Swift J. W. Three identical oscillators with symmetric coupling // Nonlinearity, 1990, vol. 3, No. 3, p. 585-601.
45. Ashwin P. Boundary of Two Frequency Behavior in a System of Three Weakly Coupled Electronic

Oscillators // Chaos, Solitons & Fractals, 1998, vol. 9, No.8, p. 1279-1287.
46. Pazo D., Sanchez E., Matias M.A. Transition to high-dimensional chaos through quasiperiodic motion // Journal of Bifurcation and Chaos, 2001, vol. 11, No. 10, p. 2683-2688.
47. Yang J. Quasiperiodicity and transition to chaos // Phys. Rev. E, 2000, vol. 61, p. 6521–6526.
48. Rompala K., Rand R., Howland H. Dynamics of three coupled van der Pol oscillators with application to circadian rhythms // Communications in Nonlinear Science and Numerical Simulation, 2007, vol. 12, No. 5, p. 794-803.
49. Maistrenko Yu., Popovych O., Burylko O., Tass P. A. Mechanism of Desynchronization in the Finite-Dimensional Kuramoto Model // Phys. Rev. Lett. 2004, vol. 93, 084102.
50. Ashwin P, King G.P., Swift J.W. Three identical oscillators with symmetric coupling // Nonlinearity, 1990, No. 3, p. 581-601.
51. Ashwin P., Burylko O., Maistrenko Y. Bifurcation to heteroclinic cycles and sensitivity in three and four coupled phase oscillators // Physica D, 2008, vol. 237, p. 454-466.
52. Karabacak O, Ashwin P. Heteroclinic Ratchets in Networks of Coupled Oscillators // J. Nonlinear Sci., 2010, vol. 20, p. 105.
53. Buskirk R.V., Jeffries C. Observation of chaotic dynamics of coupled nonlinear oscillators // Phys. Rev. A, 1985, vol. 31, p. 3332–3357.
54. Anishchenko V, Nikolaev S,, Kurths J. Bifurcational mechanisms of synchronization of a resonant limit cycle on a two-dimensional torus // Chaos, 2008, vol. 18, 037123.
55. Anishchenko V, Nikolaev S. Transition to chaos from quasiperiodic motions on the four-dimensional torus perturbed by external noise // International Journal of Bifurcation and Chaos, 2008. vol. 18, No. 9, p. 2733-2741.
56. Anishchenko V.S, Nikolaev S.M, Kurths J. Peculiarities of synchronization of a resonant limit cycle on a two-dimensional torus // Phys. Rev. E, 2007, vol. 76, 040101.
57. Anishchenko V, Astakhov S., Vadivasova T. Phase dynamics of two coupled oscillators under external periodic force // Europhysics Letters, 2009, vol. 86, p. 30003.
58. Anishchenko V, Astakhov S., Vadivasova T., Feoktistov A. Numerical and experimental study of two frequency oscillations of the external synchronization // Nonlinear Dynamics, 2009, vol. 5, p. 237-252 (in Russian).
59. Kuznetsov A., Sataev I., Turukina L. Synchronization of quasi-periodic oscillations in coupled phase oscillators // Tech. Phys. Lett., 2010, vol. 36, No. 5, p. 478-481.
60. Kuznetsov A., Sataev I., Turukina L. On the road towards multidimensional tori // Communications in Nonlinear Science and Numerical Simulation, 2011, vol. 16, p. 2371–2376.
61. Ermentrout G., Kopell N. Frequency Plateaus in a Chain of Weakly Coupled Oscillators // SIAM, J. on Mathematical Analysis, 1984, vol. 15, No. 2, p. 215-237.E-Nashar H., Cerdeira H. Geometrical properties of coupled oscillators at synchronization // Communications in Nonlinear Science and Numerical Simulation, 2011, vol. 16, No 1, p. 4508-4513.

63. Kuznetsov A., Paksyutov V., Roman Yu. Features of the synchronization of coupled van der Pol oscillators with nonidentical control parameters // Tech. Phys. Lett., 2007, vol. 33, No. 8, p. 636-638.
64. Kuznetsov A., Roman Yu. Properties of synchronization in the system of non-identical coupled van der Pol and van der Pol – Duffing oscillators. Broadband synchronization // Physica D, 2009, vol. 238, p. 54-60.

Figure captions.

Fig.1 Schematic representation of a system of three coupled self-oscillators.

Fig.2 (color on-line). Phase portraits of the system (5) for $\Delta_2 = 1.0$. *a*) $\Delta_1 = 0.5$, $\mu = 0.75$, *b*) $\Delta_1 = -0.25$, $\mu = 0.75$, *c*) $\Delta_1 = -0.25$, $\mu = 0.25$, *d*) $\Delta_1 = -1.25$, $\mu = 0.75$, *e*) $\Delta_1 = 0.75$, $\mu = 0.25$, *f*) $\Delta_1 = -1.0$, $\mu = 0.25$.

Fig.3 (color on-line). Regions of the complete synchronization of three phase oscillators *P* (red color) and quasi-periodic regimes (white color) on the parameter plane (Δ_1, μ). The lines correspond to the conditions (7) and (8). $SNP_{1,2}$ are a lines of the saddle-node bifurcation. *SNF* (saddle node fan) is a co-dimension-2 bifurcation.

Fig.4 (color on-line). Chart of the Lyapunov's exponents for the system of three coupled phase oscillators (5) for $\Delta_2 = 1$. The color palette is given and decrypted under the picture. The numbers indicate the tongues of the main resonant two-frequency regimes. These regimes are explained in the description of the Fig.5.

Fig.5 Trajectories on the phase torus. *a*) resonant two-frequency regime with winding number *w*=1:2, *b)* three-frequency regime.

Fig.6 (color on-line). *a*) The winding number chart of the system (5) in the region near of the point SNF. *b*) The fragment of the chart from Fig.*a*. Winding numbers are indicated in figure by numbers. *P* is a regime of the complete synchronization.

Fig.7 (color on-line). Charts of the Lyapunov's exponents for the system of three coupled van der Pol oscillators (1). *a*) $\lambda = 0.1$, $\Delta_2 = 0.05$, *b*) $\lambda = 0.2$, $\Delta_2 = 0.15$. *OD* is a region of "oscillator death". *PBS* is a region of partial broadband synchronization.

Fig.8 Bifurcation lines of the system (1). Values of the parameter correspond to the Fig.7a and Fig.7b. *F* is a line of the saddle-node bifurcation. *H* is a line of the Hopf bifurcation. *C* is the cusp point. *NS* is a line of the Neimark-Sacker bifurcation. *R*1 is a point of the 1:1 resonance. Line of the saddle-node bifurcation of the unstable cycle is shown by the dotted line.

Fig.9 (color on-line). Chart of the Lyapunov's exponents for the system of three coupled van der Pol oscillators (11) for $\lambda_1 = 1.3$, $\lambda_2 = 1.9$, $\lambda_3 = 1.8$, $\Delta_2 = 1.5$. *a)-d)* are phase portraits plotted at the corresponding points. *CBS* is a region of complete broadband synchronization.

Fig.10 Rotation numbers ν_{1-2} and ν_{2-3} versus the frequency detuning Δ_1 for the system (11). Values of the parameters are $\lambda_1 = 1.3$, $\lambda_2 = 1.9$, $\lambda_3 = 1.8$, $\Delta_2 = 1.5$ and $\mu = 0.32$.

Fig.11 (color on-line). Different configurations of lines of the saddle-node bifurcations and a region of the complete synchronization *P* (red color) for the system of four coupled oscillators (13). μ_c is the threshold of the complete synchronization.

Fig.12 (color on-line). *a)* Chart of the Lyapunov's exponents of the system of four coupled oscillators (13). *b*) The winding number chart for the same system. Values of the parameters are Δ_2=0.3, Δ_3=1.

Fig.13 (color on-line). Enlarged fragments of the winding numbers chart in regions near the *SNF* points. *a*) Regions near the point indicated in Fig.12*a* by the number 1. *b*) Regions near the point indicated in Fig.12*a* by the number 2. Values of the parameters are Δ_1=0.3, Δ_2=1.

Fig.14 Subdivision of the chain of four oscillators by clusters for the three types of the phase locked pair of oscillators. Parameters are chosen in such a way that the system of oscillators is near the point of the saddle-node bifurcation.

Fig.15 (color on-line). The winding number chart for the case of the co-dimension-3 bifurcation (i.e. the bifurcation of two *SNF* points merging) takes place. Values of the parameters are $\Delta_2 = 0.5$, $\Delta_3 = 1$.

Fig.16 (color on-line). Qualitative picture of the lines of saddle-node bifurcations and a region *P* of the complete synchronization (red color) for the five coupled oscillators (22). The numbers correspond to the number of equation in (24).

Fig.17 Chart of the Lyapunov's exponents for the system of five coupled phase oscillators and it's enlarged fragment, $\Delta_2 = 0.2$, $\Delta_3 = 0.9$, $\Delta_4 = 2$.

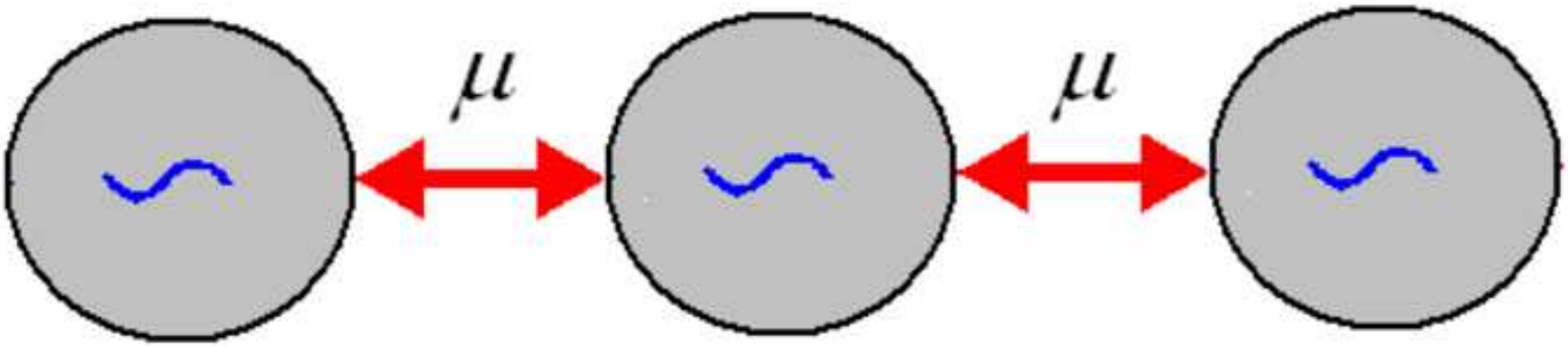
μ
μ

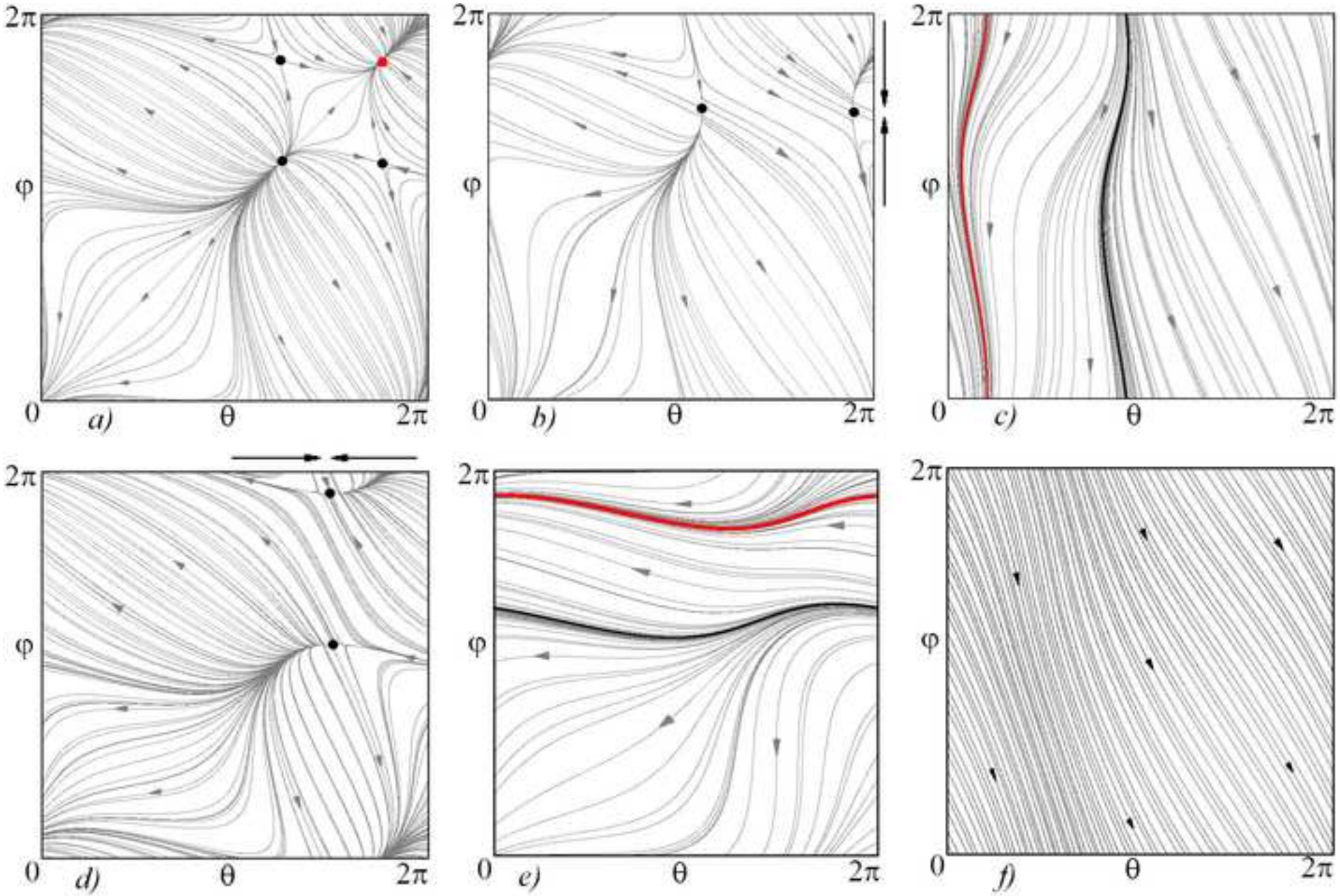
2π
φ
0
a)
θ
2π
2π
φ
0
b)
θ
2π
2π
φ
0
c)
θ
2π
2π
φ
0
d)
θ
2π
2π
φ
0
e)
θ
2π
2π
φ
0
f)
θ
2π

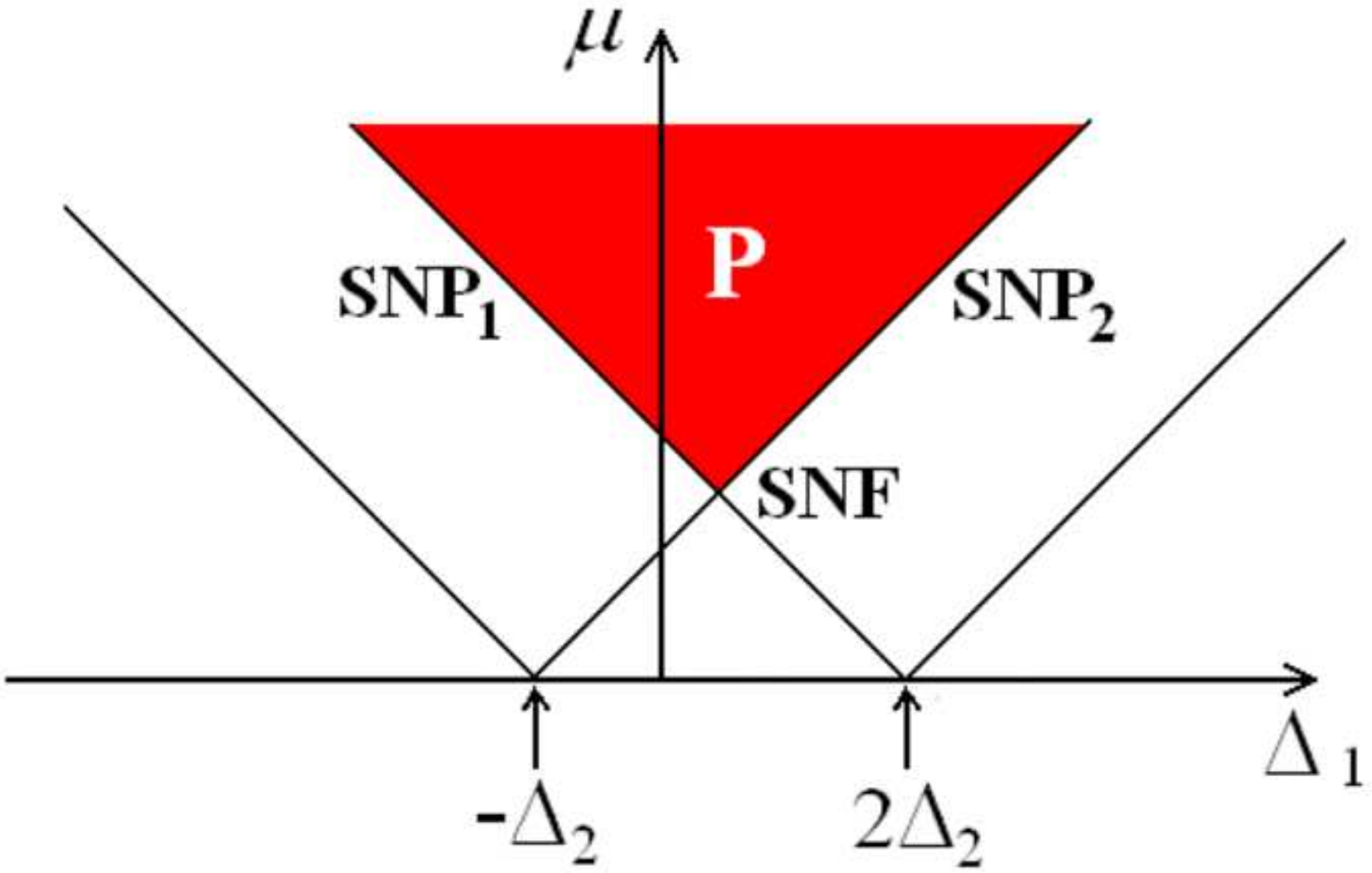
μ
P
SNP1
SNP2
SNF
Δ1
-Δ2
2Δ2

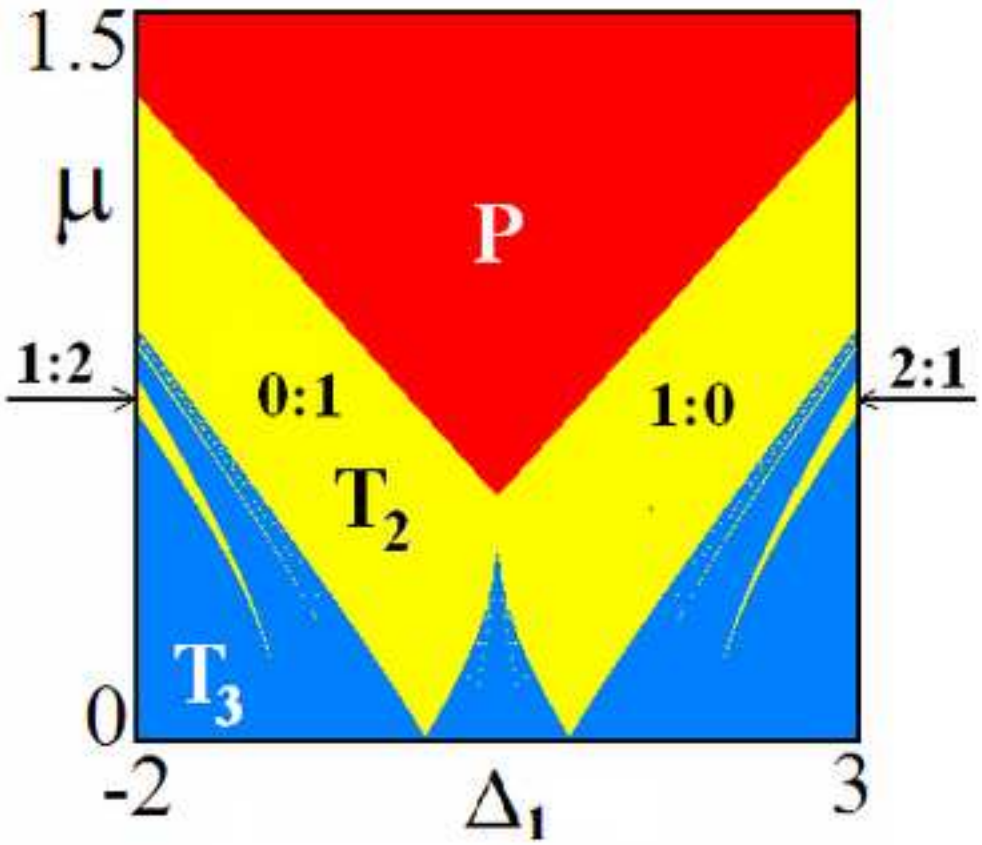

P *is the periodic regime*

T_2 *is the two-frequency quasi-periodic regime*

T_3 *is the three-frequency quasi-periodic regime*

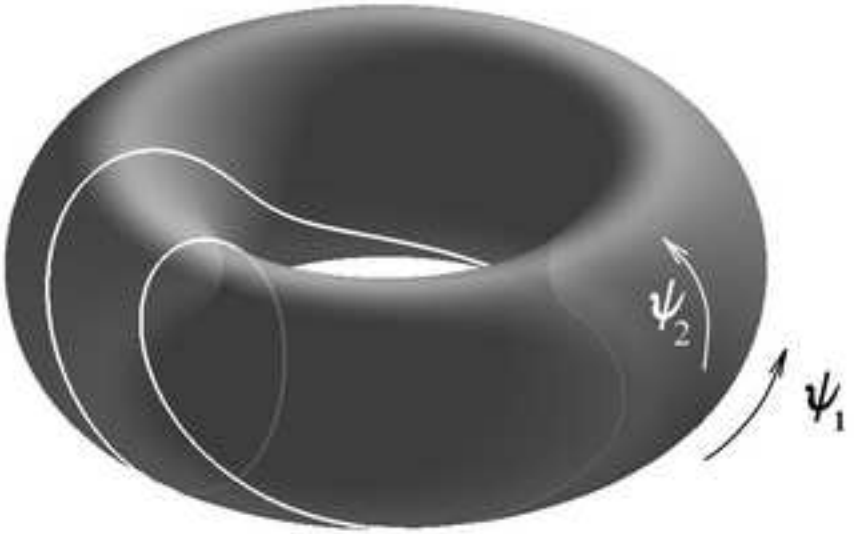

a)

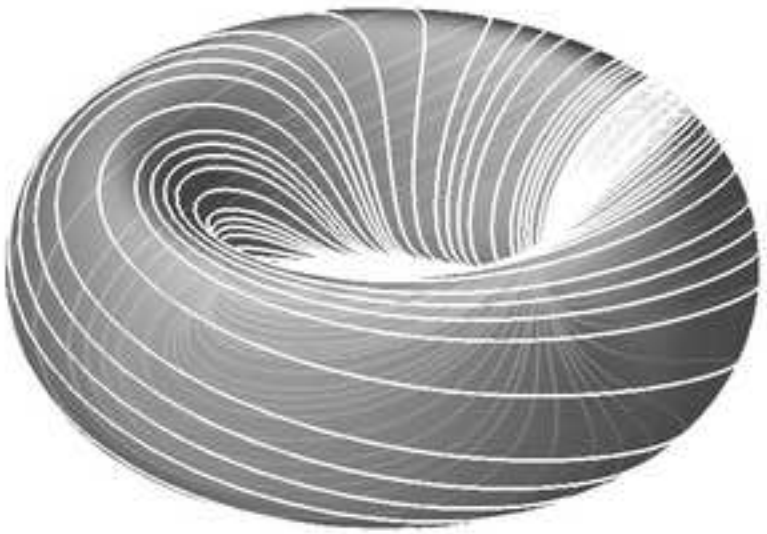

b)

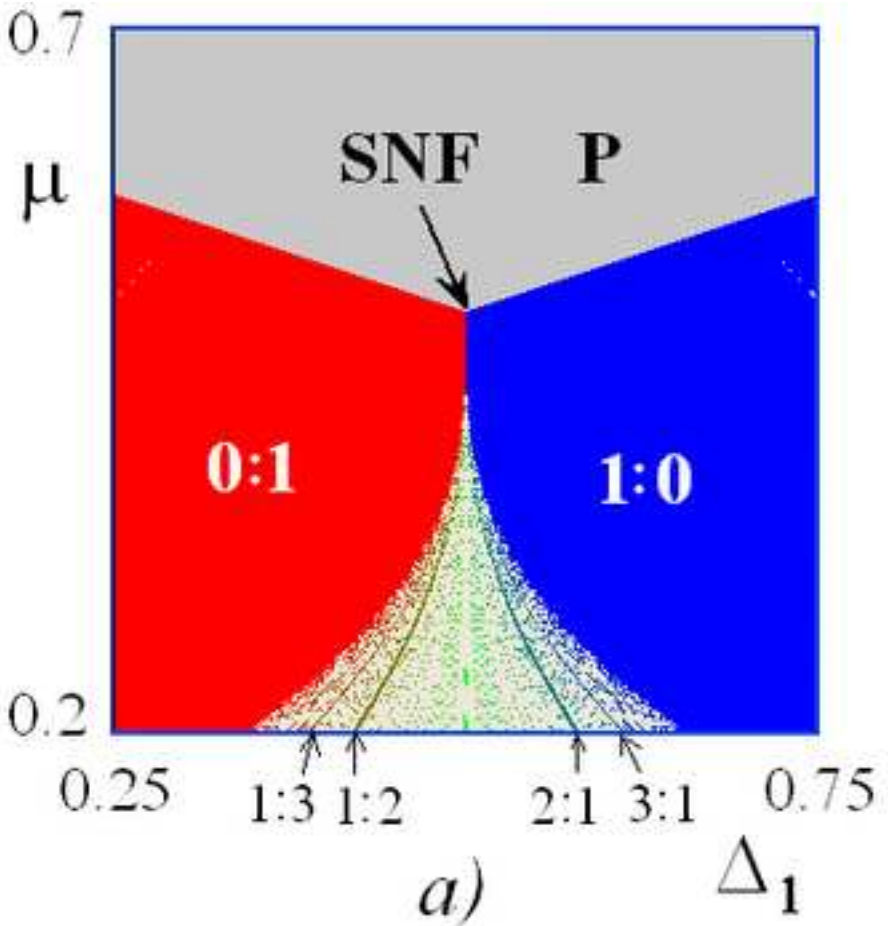
0.7
μ
SNF
P
0:1
1:0
0.2
0.25
1:3
1:2
2:1
3:1
0.75
Δ1
a)

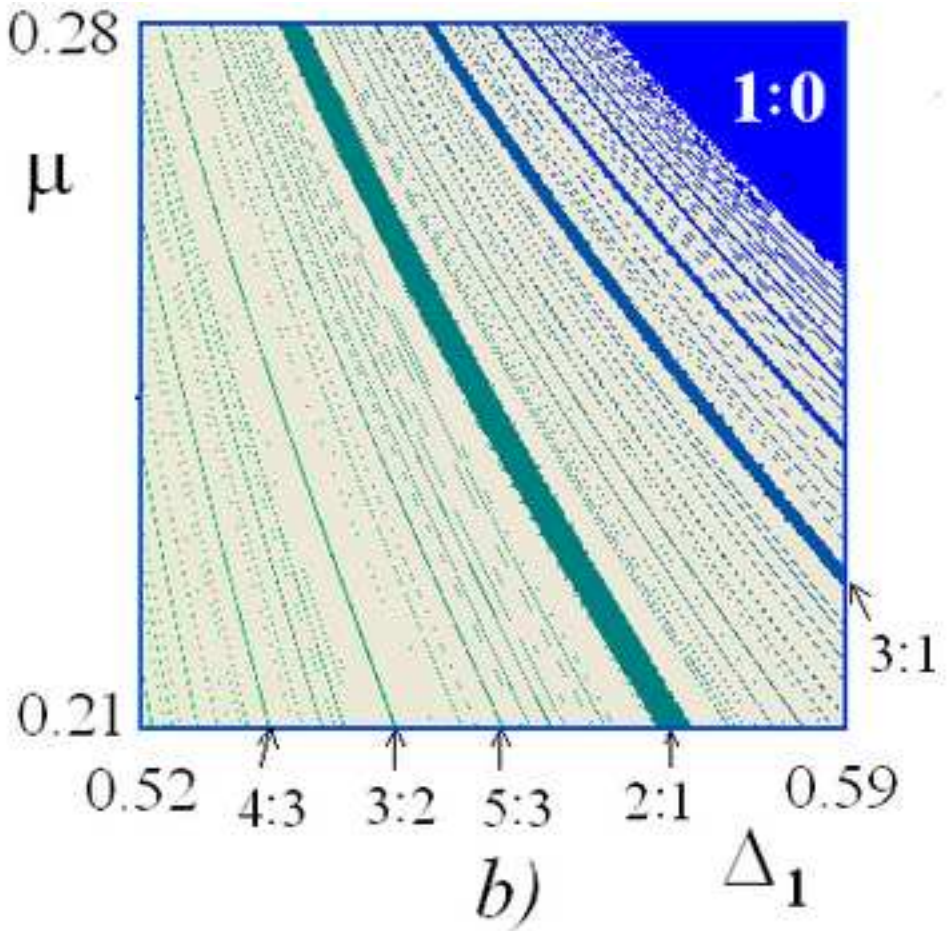
0.28
μ
1:0
3:1
0.21
0.52
4:3
3:2
5:3
2:1
0.59
Δ1
b)

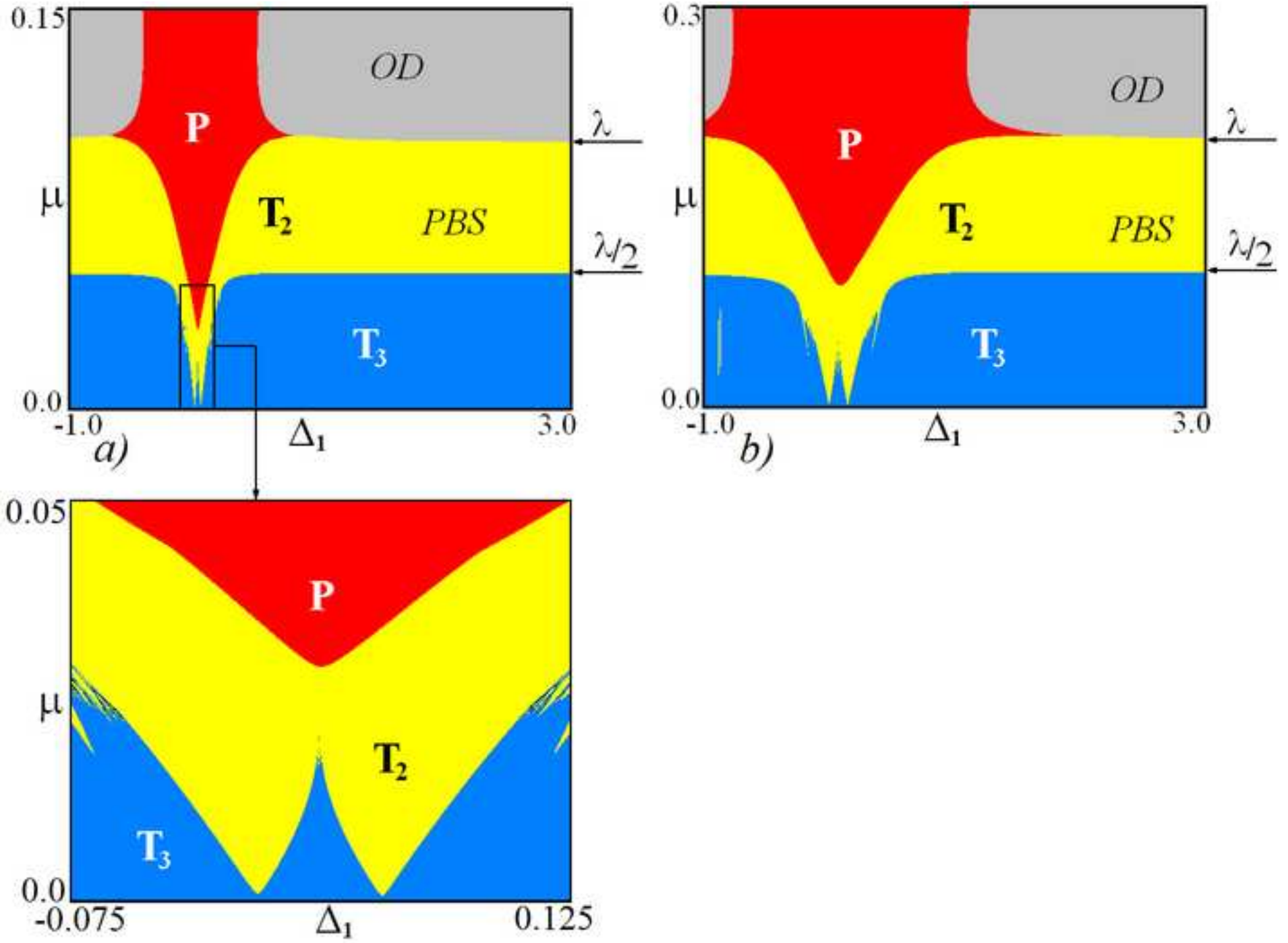
0.15
OD
P
λ
μ
T2
PBS
λ/2
T3
0.0
-1.0
Δ1
3.0
a)
0.3
OD
P
λ
μ
T2
PBS
λ/2
T3
0.0
-1.0
Δ1
3.0
b)
0.05
P
μ
T2
T3
0.0
-0.075
Δ1
0.125

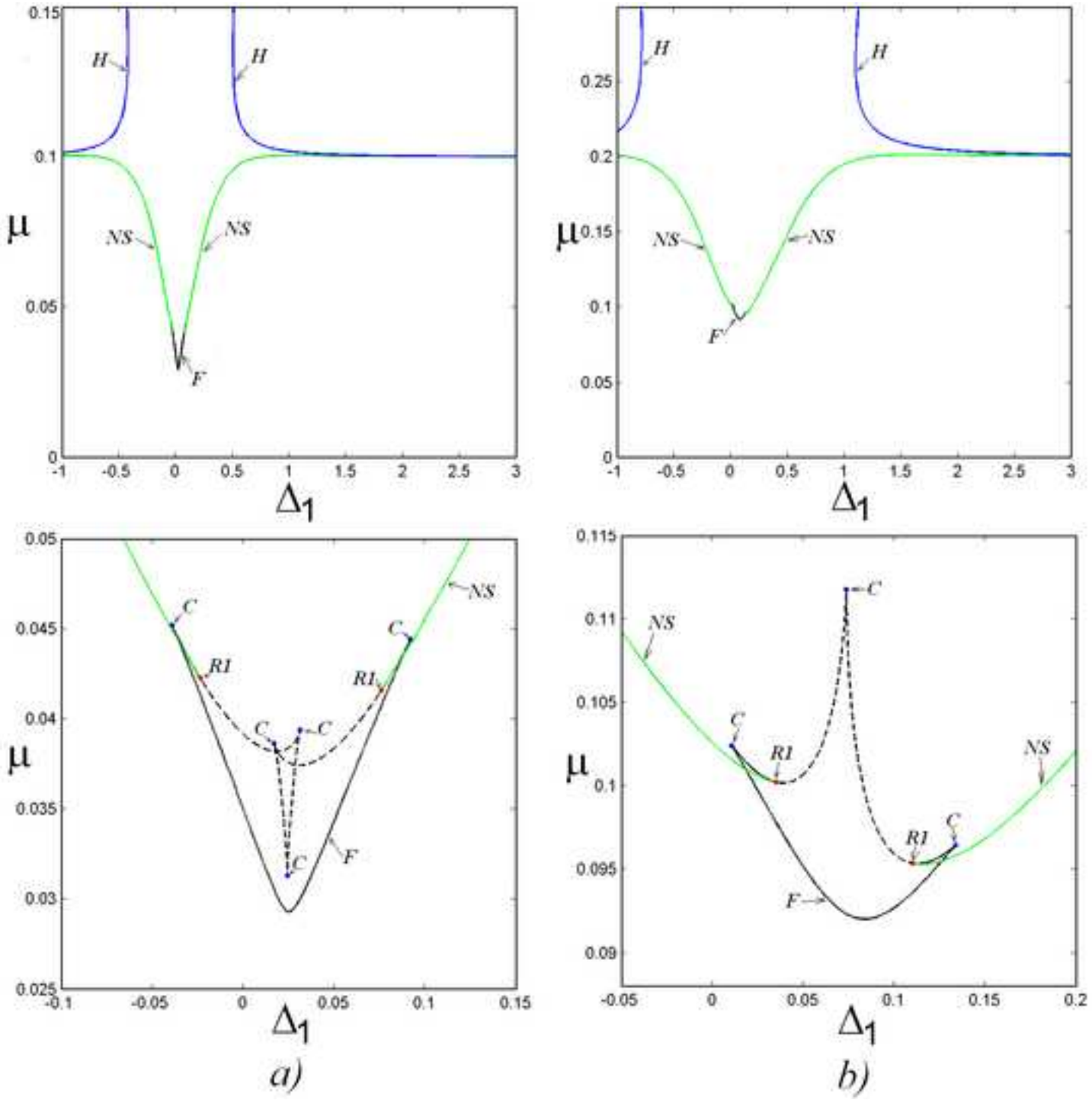
H
H
NS
NS
F
μ
Δ1
C
R1
a)
b)

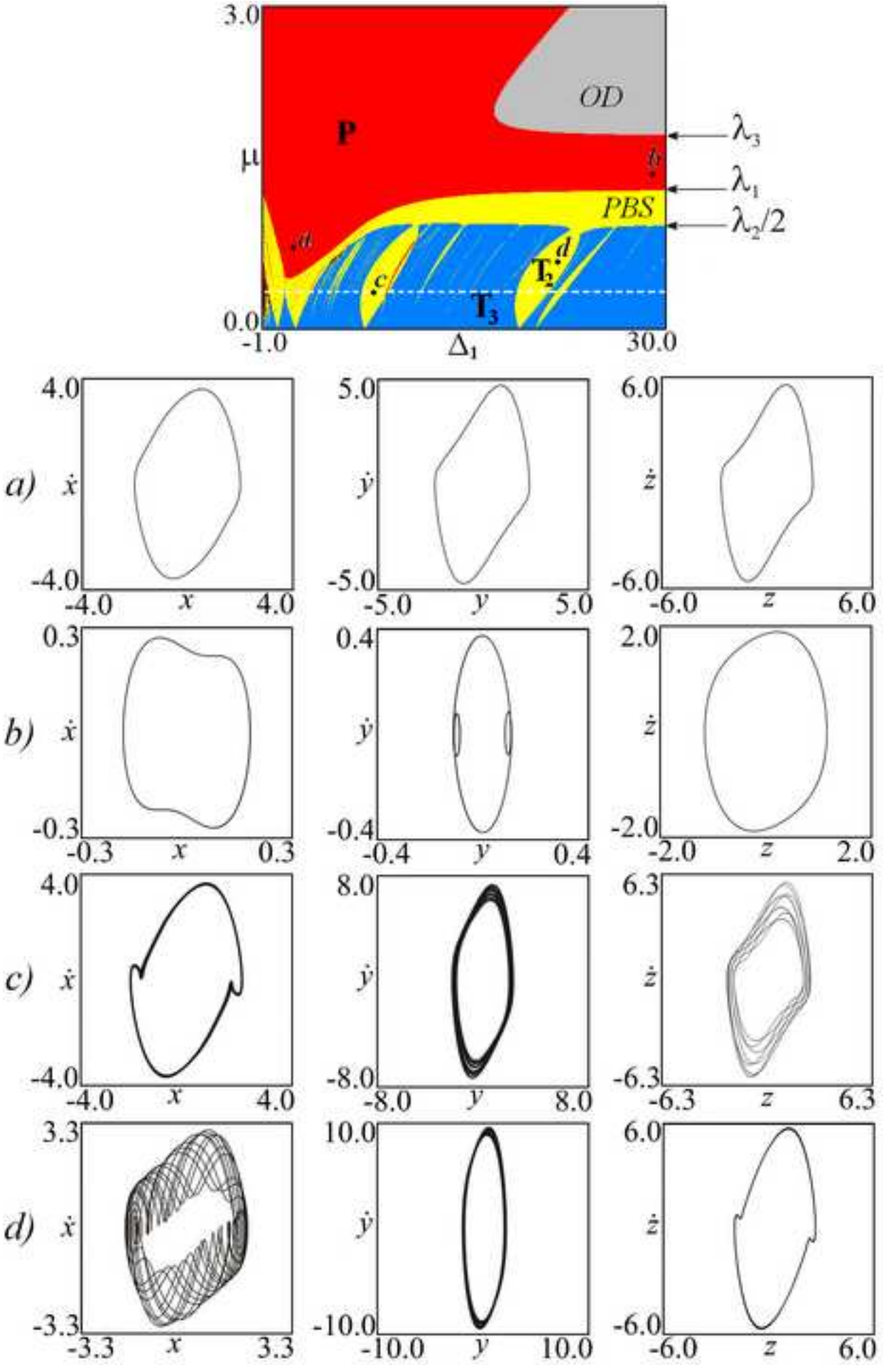
3.0
OD
P
μ
λ3
λ1
PBS
λ2/2
a
c
d
T2
T3
0.0
-1.0
Δ1
30.0
a)
b)
c)
d)
ẋ
ẏ
ż
x
y
z
4.0
-4.0
5.0
-5.0
6.0
-6.0
0.3
-0.3
0.4
-0.4
2.0
-2.0
8.0
-8.0
6.3
-6.3
3.3
-3.3
10.0
-10.0

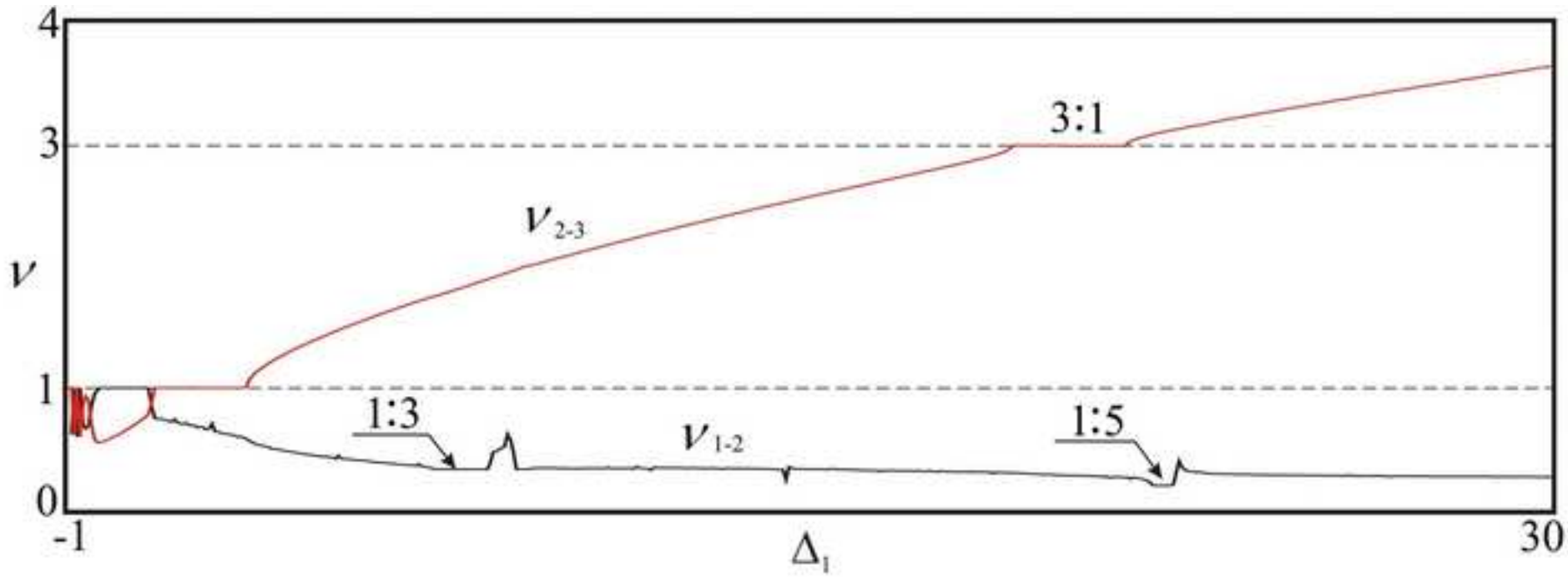
4
3
1
0
-1
30
Δ_1
ν
$\nu_{2\text{-}3}$
$\nu_{1\text{-}2}$
3:1
1:3
1:5

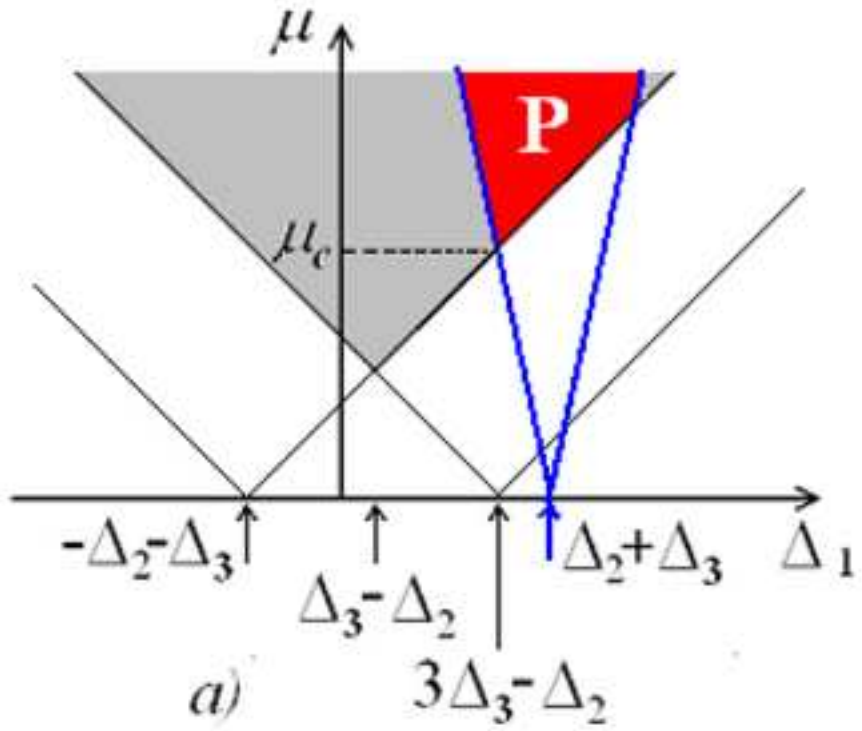
μ
P
μc
-Δ2-Δ3
Δ3-Δ2
3Δ3-Δ2
Δ2+Δ3
Δ1
a)

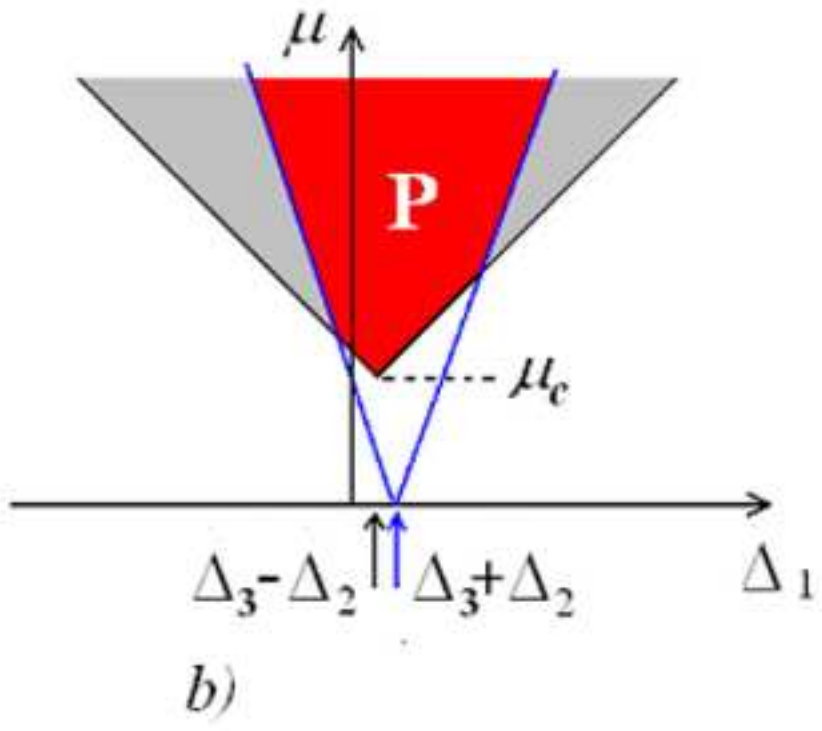
μ
P
μc
Δ3-Δ2
Δ3+Δ2
Δ1
b)

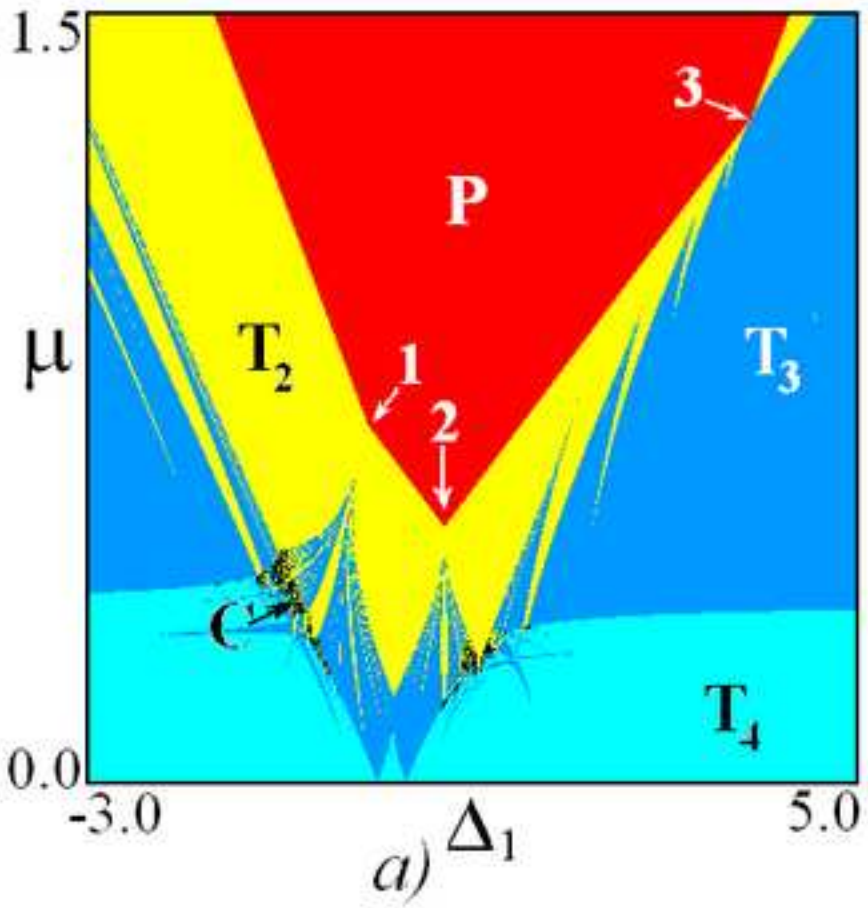

a)

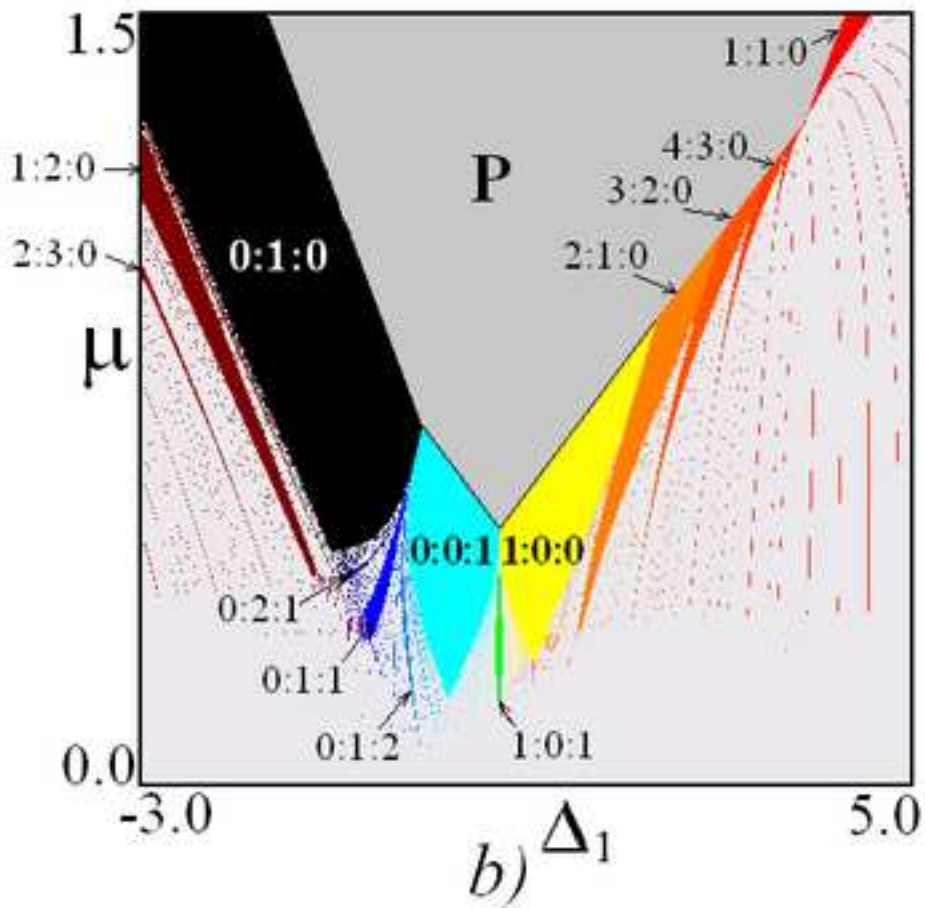

b)

T4 *is the four-frequency quasi-periodic regime*

C *is the chaos*

is the three- and four-frequency quasi-periodic regime

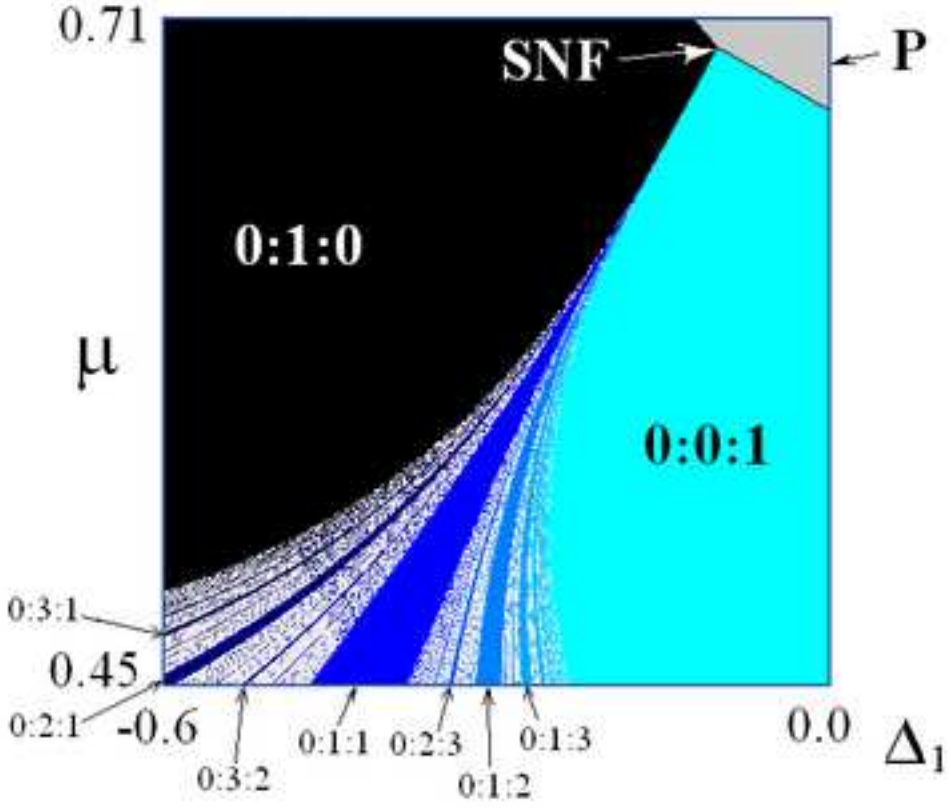
0.71
SNF
P
0:1:0
μ
0:0:1
0:3:1
0.45
0:2:1
-0.6
0:3:2
0:1:1
0:2:3
0:1:2
0:1:3
0.0
Δ1

a)

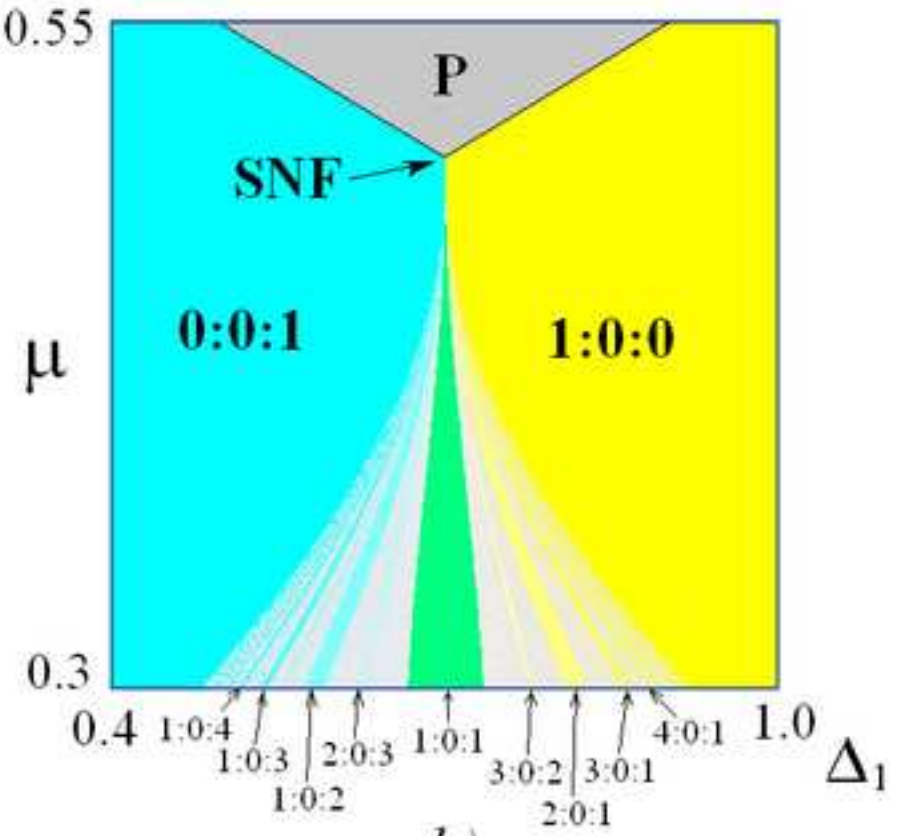
0.55
P
SNF
0:0:1
μ
1:0:0
0.3
0.4
1:0:4
1:0:3
1:0:2
2:0:3
1:0:1
3:0:2
2:0:1
3:0:1
4:0:1
1.0
Δ1

b)

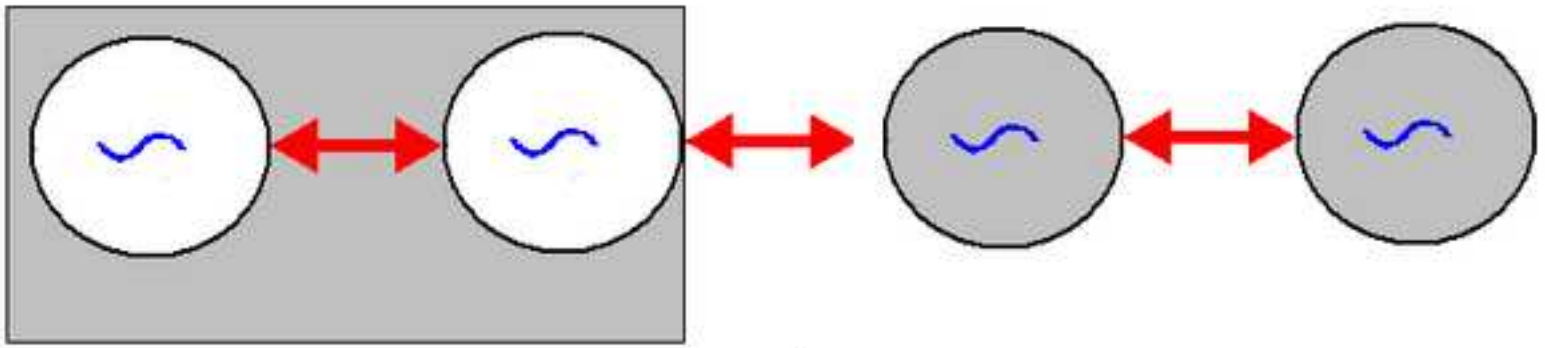

a)

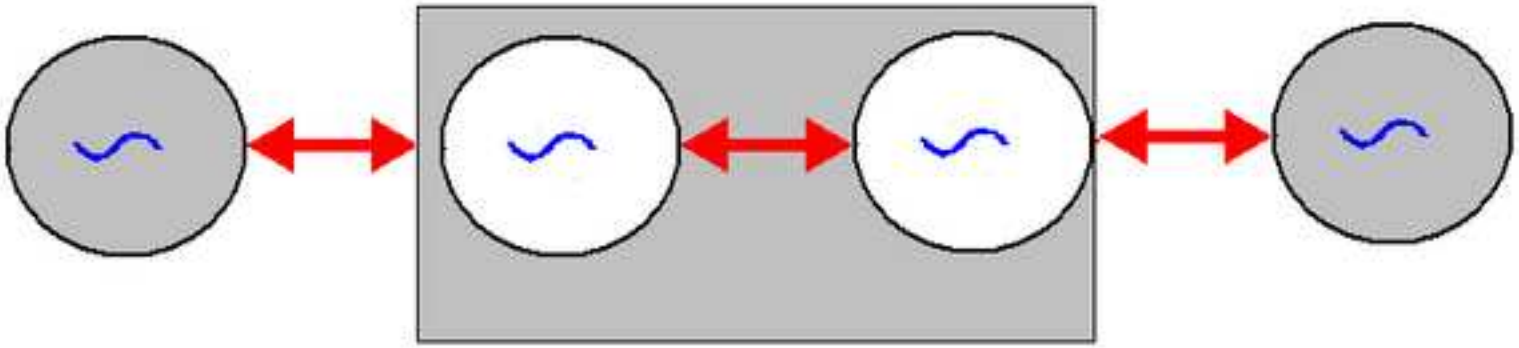

b)

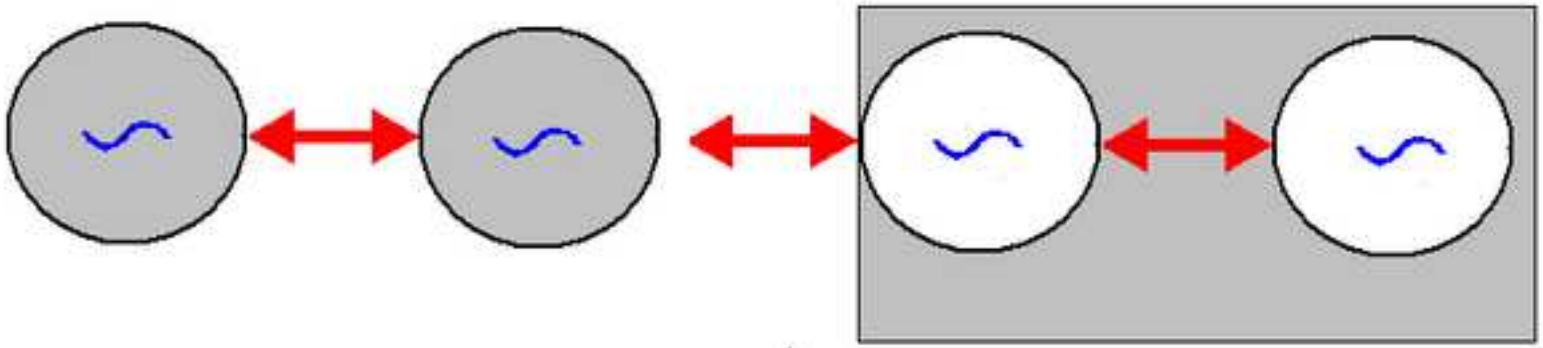

c)

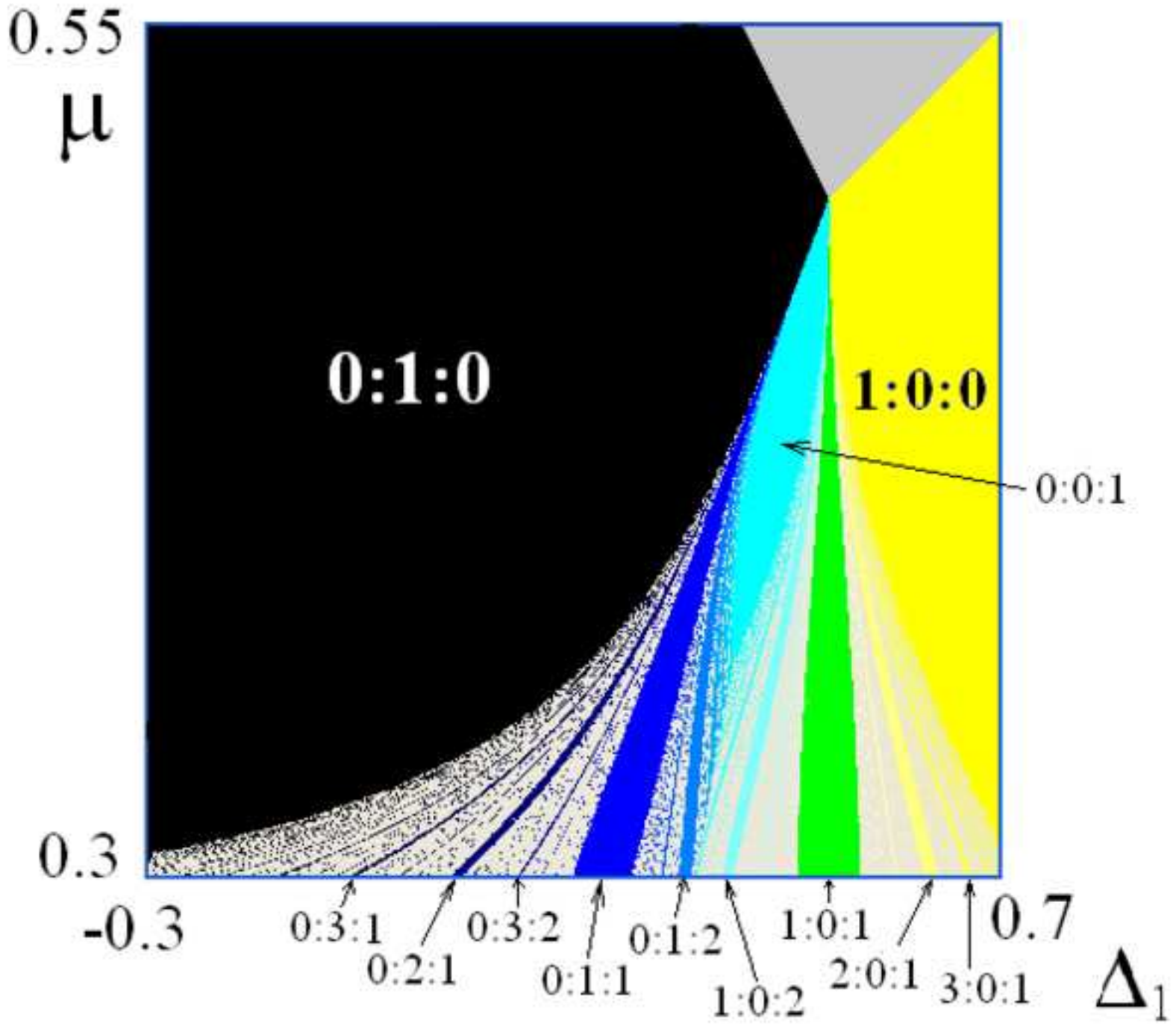
0.55
μ
0:1:0
1:0:0
0:0:1
0.3
-0.3
0:3:1
0:2:1
0:3:2
0:1:1
0:1:2
1:0:2
1:0:1
2:0:1
3:0:1
0.7
Δ1

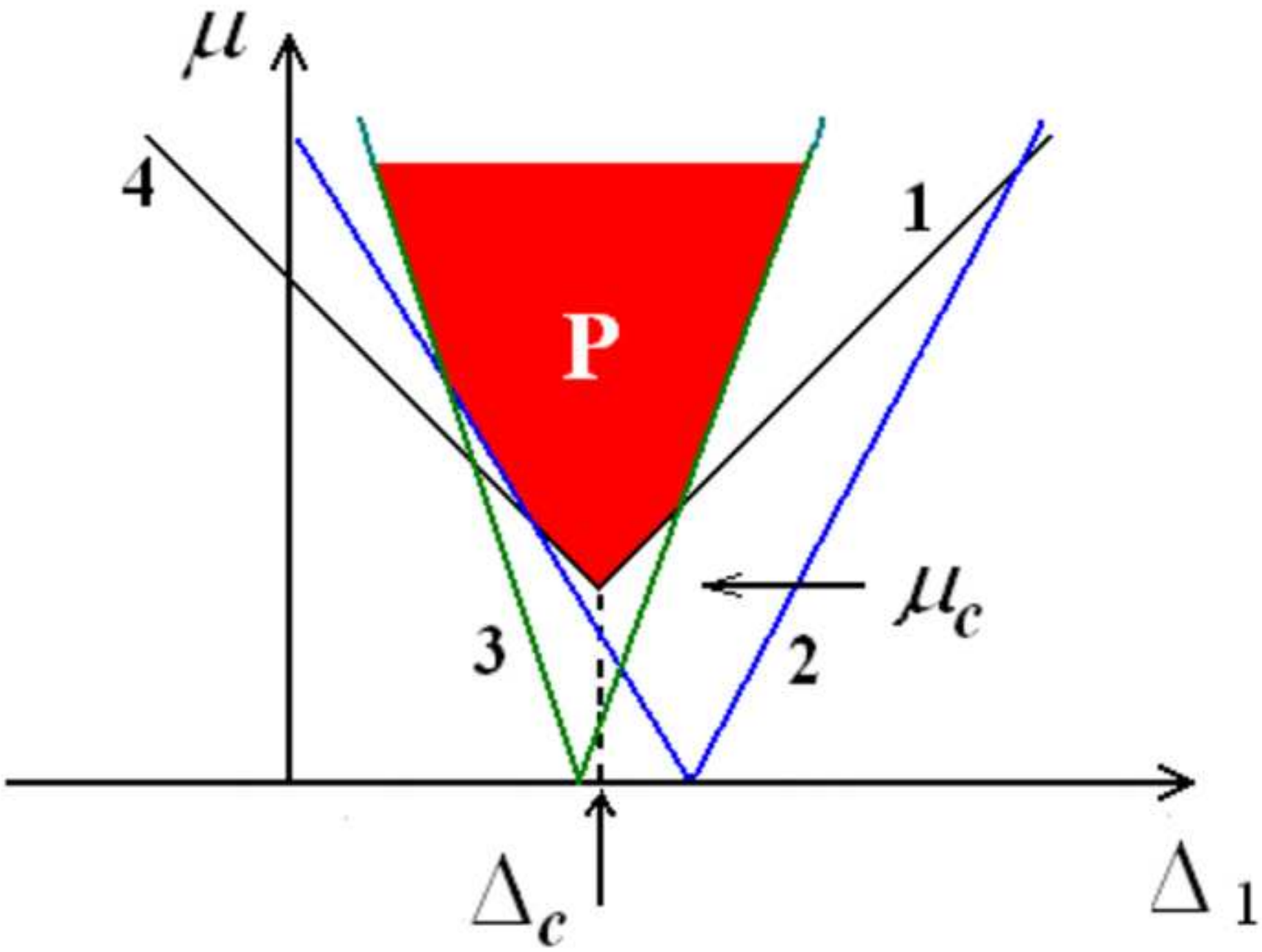
μ
4
1
P
μc
3
2
Δc
Δ1

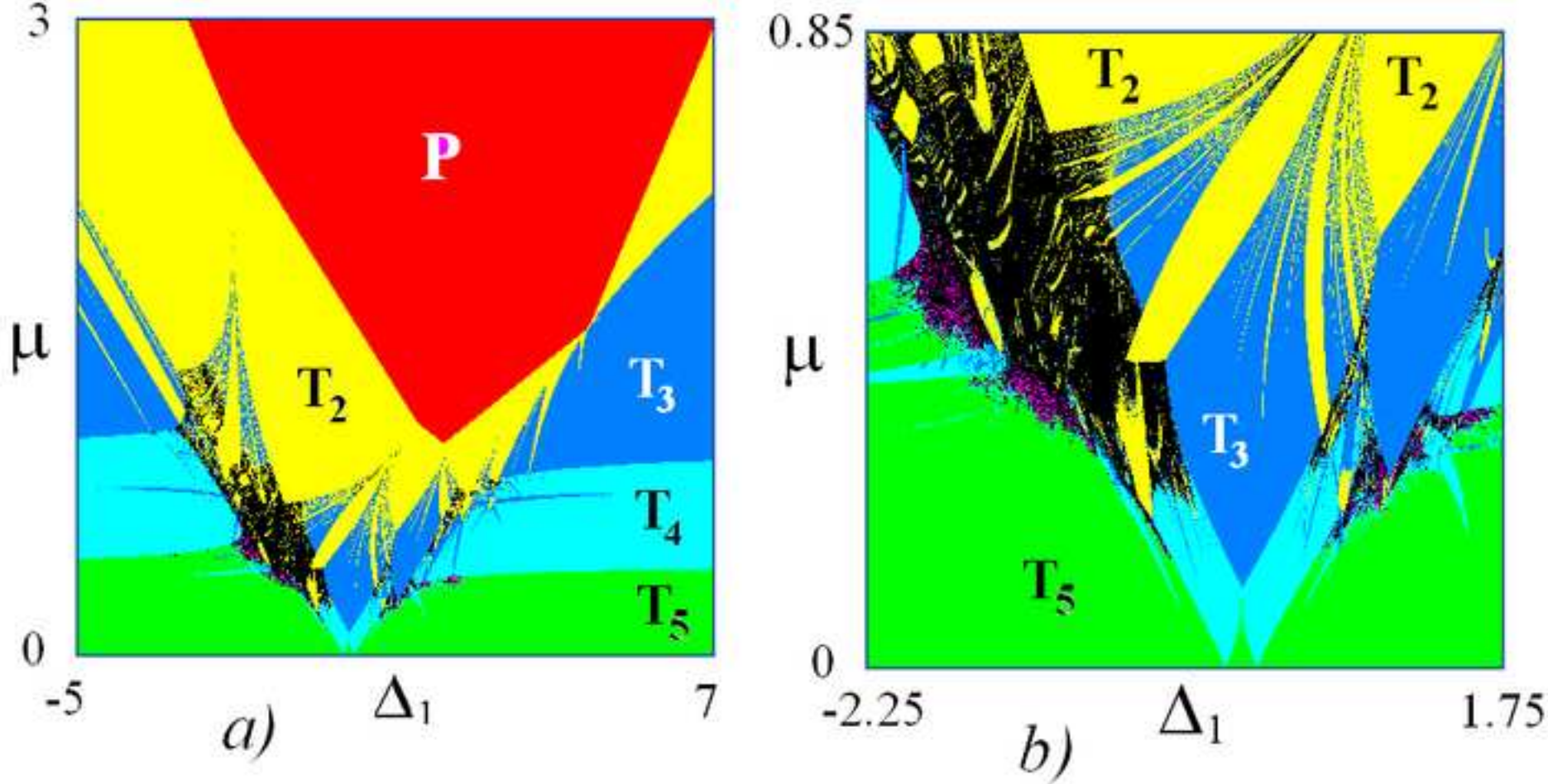
3
0
μ
-5
7
Δ1
P
T2
T3
T4
T5
a)
0.85
0
μ
-2.25
1.75
Δ1
T2
T2
T3
T5
b)